



Environnement et
Changement climatique Canada

Environment and
Climate Change Canada

The Canadian Seasonal to Interannual Prediction System version 2.1 (CanSIPsV2.1)

Technical Note

Canadian Meteorological and Environmental Prediction Centre

H. Lin¹, R. Muncaster¹, G.T. Diro², W. Merryfield³, G. Smith¹, M. Markovic¹,
A. Erfani², S. Kharin³, W.-S. Lee³, R. Parent², R. Pavlovic², M. Charron¹

¹-Meteorological Research Division

² Canadian Meteorological and Environmental Prediction Centre

³-Canadian Centre for Climate Modelling and Analysis (CCCma)

30 November 2021

Table of Contents

1	Introduction.....	4
2	Modifications to models	7
2.1	CanCM4i.....	7
2.2	GEM5-NEMO	7
3	Forecast initialization.....	8
3.1	CanCM4i.....	9
3.2	GEM5-NEMO	9
4	Reforecasts.....	10
4.1	CanCM4i.....	10
4.2	GEM5-NEMO	10
5	Systematic errors	12
6	Skill evaluation of CanSIPSv2.1 comparing to CanSIPSv2	17
6.1	Surface air temperature	17
6.2	Precipitation	21
6.3	500-hPa geopotential height	24
6.4	SST and ENSO	27
6.5	MJO	30
6.6	Sea ice.....	30
6.7	Snow water Equivalent and soil moisture	32
7	Qualitative evaluation of the parallel run	33
8	Details of implementation	34
9	Summary.....	36
10	Acknowledgements	36
11	References	38
	Appendix A List of Acronyms.....	43

1 Introduction

In September 1995 CMC began issuing forecasts for seasonal mean near-surface temperatures and accumulated precipitation in Canada using a two-model ensemble dynamical prediction system based on the first Historical Forecast Project, or HFP (Derome et al. 2001). These forecasts for the standard seasons DJF, MAM, JJA and SON were issued four times per year on December 1, March 1, June 1 and September 1. Initially the two component atmospheric circulation models, each with six ensemble members, were CCCma's AGCM2 (McFarlane et al. 1992), and the SEF global spectral model developed at Recherche en prévision numérique (RPN; Ritchie, 1991), whereas the GEM model (Côté et al. 1998) developed at RPN replaced the SEF model in March 2004.

CMC began issuing longer-lead statistical forecasts for seasonal mean near-surface temperatures and accumulated precipitation in Canada in late 1996. These forecasts, at lead times of three, six and nine months, were based on application of Canonical Correlation Analysis (CCA) with seasonal means of sea surface temperature (SST) and 500-mb geopotential height over the preceding 12 months as predictors (Shabbar and Barnston 1996). The seasons forecast by this system were the same as the zero-lead dynamical forecasts (except with longer lead) and the dates of issuance were also the same.

The CMC's dynamical seasonal forecast system underwent a major upgrade in October 2007 to a four-model system using AGCM2, SEF, GEM and CCCma's AGCM3 (Scinocca et al. 2008) with total of 40 ensemble members, 10 from each model. From the beginning, each 10-member model ensemble was constructed from 24-h lagged initial conditions covering the 10 previous days of the forecast initiation. That period was reduced to 5 days in 2008 by using 12h lags. Seasonal forecasts were issued both at zero-month lead (months 1-3) and one-month lead (months 2-4) on the first day of every month, and a first-month forecast for surface temperature only was issued on the 1st and 15th of every month. Hindcasts for bias correction and skill assessment were provided by the second Historical Forecasting Project (HFP2; Kharin et al. 2009). The CCA-based longer-lead forecasts continued to be issued four times per year.

The main basis for skill in a dynamical seasonal forecasting system is its ability to model the atmospheric response to relatively slowly varying boundary conditions, primarily anomalies in sea surface temperature (SST). Because all the models comprising the HFP and HFP2 systems are atmospheric circulation models with no dynamical ocean, future SSTs in these forecasts had to be prescribed, based on information available at the beginning of the forecast. Although there are numerous possible choices for such a prescription, in the HFP and HFP2 systems SSTs during the forecast periods were specified to be the mean SST anomalies during the 30 days preceding the forecast, added to the seasonally varying SST climatology. Of course, a serious limitation of this prescription of anomaly persistence is that actual SST anomalies evolve with typical time scales of a few months, so that the prescribed SST anomalies at the end of the forecast may not resemble the actual SST anomalies at that time. This limits the utility of such “two-tier” forecast systems beyond forecast periods of a few months, and indeed the HFP forecasts were limited to three months and the HFP2 forecasts to four months for this reason.

The two-tier seasonal forecast system was replaced by the Canadian Seasonal to Interannual Prediction System (CanSIPS) in December 2011, which is a global coupled one-tier system. The first version of CanSIPS used two atmosphere-ocean coupled climate models, CanCM3 and CanCM4, that were developed at CCCma, with a total of 20 ensemble members, 10 from each model. From the beginning of each month, 10 ensemble members of forecast for each model were produced for 12 months from initial conditions of small perturbations at the same time, i.e., with a burst start approach. Details on the first CanSIPS system are described in Merryfield et al. (2013).

It is noteworthy to point out that CanSIPS has been an integral part of several international activities related to multi-model ensemble seasonal forecasts, including the North American Multi-model Ensemble (NMME) (e.g., Kirtman et al. 2014), the WMO Long-Range Forecast Multi-Model Ensemble (e.g., Kim et al. 2015), the multi-model climate prediction of the Asian-Pacific Economic Cooperation Climate Center (APCC) (e.g., Min, et al. 2014) and recently joined Copernicus Climate Change Services (C3S).

From September 1995 to June 2015, output of the first month from the seasonal forecast system was used to produce the 30-day-averaged temperature anomaly forecast, which was the only monthly forecast product in Canada. Since July 2015, the monthly forecast is produced in CMC based on the Global Ensemble Prediction System (GEPS; Gagnon et al. 2015), which takes advantage of the increased resolution and improved initialization of GEPS (Lin et al. 2016).

The second version of CanSIPS (CanSIPSV2) is a multi-model ensemble seasonal prediction system that became operational in July 2019. CanSIPSV2 is composed of two global coupled models (GEM4-NEMO and CanCM4i). GEM4-NEMO is an NWP-based global atmosphere (GEM)-ocean (NEMO)-sea ice (CICE) coupled model. CanCM4i is an upgraded version of CanCM4 with improved ice initialization. GEM4-NEMO replaced CanCM3 in CanSIPS and was combined with CanCM4i to form the second version of CanSIPS for multi-model ensemble seasonal prediction. Development of GEM4-NEMO seasonal forecast model took place mainly at RPN, exploiting the coupled model and modeling expertise available there, which also benefits from the contribution of the CONCEPTS project.

More recently, GEM4-NEMO, one component of CanSIPSV2, has undergone improvement in model version and configuration into GEM5-NEMO to form CanSIPSV2.1. This document describes the updates in the Canadian Seasonal to Interannual Prediction System (CanSIPSV2.1). In Sections 2 we present modifications to the prediction components of CanSIPS in support of the operational implementation of November 30, 2021 to replace CanSIPSV2. Section 3 describes the forecast initialization. The reforecast is introduced in Section 4. Section 5 describes systematic errors in CanCM4i and the updated GEM5-NEMO. Skill evaluation results are presented in Section 6. Section 7 gives evaluation of the parallel run. The detail of implementation is given in Section 8. Finally, we summarize results in Section 9.

The current implementation represents cumulative efforts of many people not only from the CanCM4i and GEM5-NEMO teams, but also from other groups such as the modelling and post-processing sections in research and development divisions, and operational sections of Environment and Climate Change Canada (ECCC) co-located at the Canadian Meteorological Centre (CMC) in Dorval, Québec

2 Modifications to models

Like its predecessors (the HFP, HFP2, CanSIPS, and CanSIPSV2), CanSIPSV2.1 is a multi-model system which takes advantage of the generally greater skill of multi-model compared to single-model systems for a given ensemble size (e.g. Kharin et al. 2009).

CanSIPSV2.1 consists of two global coupled models, CanCM4i and GEM5-NEMO. CanCM4i is the same model version used in CanSIPSV2. This model is described in detail in Merryfield et al. (2013), so only its most basic aspects are outlined here. On the other hand, GEM5-NEMO is an improved version of GEM4-NEMO model introduced to CanSIPSV2.1 and will be described in detail here.

2.1 CanCM4i

CanCM4i couples CCCma's fourth-generation atmospheric model CanAM4 to CCCma's CanOM4 ocean component. Atmospheric horizontal resolution is T63, corresponding to a 128×64 Gaussian grid, with 35 vertical levels and a top at 1 hPa. The 256×192 grid of CanOM4 provides horizontal resolution of approximately 1.4 degrees in longitude and 0.94 degrees in latitude, with 40 vertical levels. Version 2.7 of the CLASS land surface scheme and a single-category, cavitating-fluid sea ice model are employed, both formulated on the atmospheric model grid.

2.2 GEM5-NEMO

GEM5-NEMO, like its predecessor GEM-NEMO, is developed at the Recherche en Prévision Numérique (RPN), is a fully coupled model with the atmospheric component of GEM (Côté et al. 1998) and the ocean component of NEMO (Nucleus for European Modelling of the Ocean, <http://www.nemo-ocean.eu>).

The GEM version used is 5.1.0, with a horizontal resolution of about 1x1degree on a Yin-Yang grid, and 85 vertical levels with the top at 0.1 hPa. The land scheme is ISBA (Noilhan and Planton, 1989; Noilhan and Mahfouf, 1996), where each grid point is assumed to be independent (no horizontal exchange). The modified atmospheric deep convection parameterization scheme of Kain-Fritsch (Kain and Fritsch 1990) is used. The Bechtold scheme (Bechtold et al. 2001) is

applied for shallow convections. The model allows for vegetation and ozone seasonal evolutions during the integration. In GEM5, all greenhouse gases are evolved using input files and are updated through the simulation. This is different from the predecessor where a linear trend of CO₂ is specified in the computation of the evolution of anthropogenic radiative forcing. The GEM model is integrated with a time step of 30 minutes. Unlike its predecessor, the current system uses implicit surface flux scheme for all members. However, to account for model uncertainty, GEM5 uses stochastic perturbation of parameters (SPP), which includes perturbations in 18 parameters whose values and ranges are determined based on simulated climatology and variability (e.g., tropical waves) as well as forecast skill.

The ocean model NEMO is NEMO 3.6 ORCA 1 with a horizontal resolution of $1^\circ \times 1^\circ$ (1/3 degree meridionally near the equator) and 50 vertical levels. The CICE 4.0 (Community of Ice Code, Hunke and Lipscomb 2010) model is used for the sea-ice component with five ice categories. The NEMO model is run with a 30-minute time step. Compared to its predecessor, GEM5-NEMO has incorporated the following updates. The ice physics parameters are modified, in particular Z0_seaice/iceruf has been changed from 1.6e4 to 5.4e4. The bug that was found in the ice velocity exchange between NEMO and GEM is also fixed. It has to be noted that GEM5-NEMO is using CONCEPTS version 5.3.0, which is an upgrade from CONCEPTS 3.1.3.

GEM and NEMO are coupled once every half an hour through the GOSSIP coupler. No flux corrections are employed in the coupled model.

3 Forecast initialization

Similar to what was done in CanSIPSv2, each of the two models in CanSIPSv2.1, perform a 12-month long forecast once a month, initialized at the beginning of each month (hindcast) or the last day of the previous month (in real time forecast). They also perform a 6 month long forecast on the 15th of each month. For all other dates, CanSIPS performs a 1-month forecast. Each model produces forecasts of 10 ensemble members with all the integrations starting from the same date. However, the two models take different approaches in the initialization for the forecasts.

3.1 CanCM4i

Each CanCM4i ensemble member is initialized from a separate assimilating model run in which atmospheric temperature, moisture, horizontal winds, SST and sea ice concentration are constrained by values from the Global Deterministic Prediction System (GDPS) analysis. Land surface variables are initialized from output of land-atmosphere coupled model with atmospheric fields are nudged towards the (re)-analysis fields during the assimilating model runs, whereas subsurface ocean temperatures are constrained by values from the Global Ice Ocean Prediction System (GIOPS) analysis through an offline procedure. Details of the initialization methods are provided in Merryfield et al. (2013). The initial conditions for Northern Hemisphere (Arctic) sea ice thickness are obtained from the SMv3 statistical model of Dirkson et al. (2017). (Additional changes in reforecast initialization to improve consistency between reforecasts and real-time forecasts are described in section 4.).

3.2 GEM5-NEMO

In the forecast, the atmospheric initial conditions of GEM5-NEMO come from those of the Global Ensemble Prediction System (GEPS; Gagnon et al. 2015), that are generated from EnKF with data assimilation. Ten of the GEPS perturbed initial conditions are used for the GEM5-NEMO seasonal forecast.

For the land surface initial conditions, in addition to taking advantage of the CMC analysis one important consideration is to make it consistent with the reforecast. In the reforecast, which will be introduced in section 4.2, we initialize the land surface by running the Surface Prediction System or SPS (Carrera et al. 2010) forced by the near-surface atmospheric and the precipitation fields of the ERA-5 reanalysis. In the real-time forecast, the land surface initial fields are generated by forcing the SPS with the CMC analysis. One important change in the current land initialization procedure is the configuration of SPS. SPS is now configured in such a way that the forcing fields are given in the lowest model level as opposed to the diagnostic level used in the previous version of GEM4-NEMO. This has resulted improvements in the simulated land surface variables such as snow water equivalent (SWE).

The ocean and sea ice initial conditions in the forecast come from the CMC GIOPS analysis (Smith et al. 2016). The near surface air temperature from GEPS and the snow depth from SPS are used

for the initialization of these variables over sea ice in CICE. For the reforecast, the ocean and sea ice initial conditions are described in section 4.2. All ensemble members have the same ocean and sea ice initial conditions.

4 Reforecasts

For seasonal predictions, model drift and systematic model errors become a serious problem that contaminates the forecast quality. A common practice in seasonal prediction is to perform a historical reforecast (or hindcast) to estimate the model climatology and statistics, so that calibrated anomaly forecasts can be made. Another purpose of the reforecast is to generate a long record of forecast data to quantify the performance of the forecast system. Therefore, the reforecast is an important component of the seasonal forecast system. As in CanSIPSV2, the reforecast is made with each individual model, covering 41 years from 1980-2020 with 10 members of 12-month integration starting from the beginning of each month. In the reforecast, each individual model has the same configuration as in the forecast.

4.1 CanCM4i

In CanCM4i, modelled sea ice thickness is constrained near values from the SMv3 statistical model of Dirkson et al. (2017), which is much more realistic than the stationary model-based climatology employed for CanCM4, in part because it accounts for the long-term thinning of Arctic sea ice. Modelled sea ice concentration is constrained near values from the Had2CIS product described in section 4.2. Had2CIS provides improved temporal consistency across the reforecast period, as well as improved consistency with sea ice concentrations from the GDPS analysis used in real time, compared to the concentration product used to initialize CanCM4 reforecasts. Finally, initial subsurface ocean temperatures are constrained by the ORAP5 ocean reanalysis (Zuo et al. 2015), which is both closer in its formulation to the GIOPS analysis used in real time, and has more realistic trends than the ocean reanalysis used to initialize CanCM4 reforecasts.

4.2 GEM5-NEMO

In the reforecast, the atmospheric conditions are initialized using the ERA-5 reanalysis (Hersbach et al., 2020). Random isotropic perturbations are added to the reanalysis fields to create 10

different initial conditions. The atmospheric perturbations are homogeneous and isotropic as in Gauthier et al. (1999). Only the stream function and the unbalanced temperatures are perturbed as in EnKF (see Houtekamer et al., 2009). These perturbed fields are then transformed to wind, temperature and surface pressure.

The ocean initial fields come from the ORAS5 ocean reanalysis (Zuo et al. 2019). The monthly values of temperature, salinity, sea surface height, zonal and meridional currents are interpolated to daily values. The sea ice concentration initial fields are the Had2CIS, which was prepared by Woo-Sung Lee of CCCma, who combined the digitized sea ice charts from the Canadian Ice Service (CIS) with the HadISST2.2. The original HadISST2.2 employs an ice chart-based bias correction of the passive microwave record (Titchner and Rayner 2014). The monthly HadISST2.2 data, the digitized CIS weekly sea ice charts over the Arctic region and the weekly CIS "Great Lakes ice charts" over Great Lakes are interpolated to daily data before the combination. The sea ice thickness is interpolated from the monthly ORAS5 data. It must be noted that Had2CIS data extends until the end of 2015. After 2015 the ice concentration comes from GIOPS analysis (as is done in the initialization of the forecast). The ice thickness, however, continues to come from ORAS5. This implies that after 2015, the ice concentration and ice thickness are coming from different sources. A pre-processing is performed to remove all ice where either the ice concentration or ice thickness is below a minimum threshold value. If a grid point exists where there is a significant ice concentration but no ice thickness value (ORAS5 generally has a smaller ice extent than GIOPS), a climatological thickness is provided. The near surface air temperature from perturbed ERA-5 reanalysis and the snow depth from SPS are used for the initialization of these variables over sea ice in CICE.

For the land surface initialization, we make use of historical dataset of surface fields produced by SPS (Carrera et al. 2010). It is previously known as GEM-surf and it was used in several studies at high resolution (see Separovic et al. 2014, Ioannidou et al. 2014 and Bernier and Bélair 2012). To generate more realistic land surface conditions, we have run the SPS for the period 1980-2020 to create surface fields compatible with the surface scheme of the model. The SPS is simply the surface schemes (land, sea ice and glacier) of the GEM model used in offline mode. To initialize the land surface fields in the reforecast, we have forced SPS by the near-surface (lowest model level) atmospheric and the precipitation fields coming from the ERA-5 reanalyses. The surface

pressure, the 2-m temperature and dew-point depression as well as the solar and infra-red downward radiative fluxes at the surface are provided to SPS at a 1-hour interval. To limit the snow accumulation over glaciers, the maximum snow depth is set to 12 meters in the initial condition.

5 Systematic errors

In this section, the systematic error is analyzed for the CanCM4i and GEM5-NEMO models, which is the difference between the predicted and observed climatology over the reforecast period of 1981-2010. The objective is to demonstrate the general behavior of the two models related to model drift. When doing seasonal prediction, forecasts of anomalies are produced, where the model climate estimated from the reforecast is subtracted, and the systematic error is removed in the forecast. It thus appears that there is no direct impact of the systematic error on the forecast skill, which will be presented in the next section. However, the systematic error does affect the forecast skill through the model dynamics. For example, a biased middle-latitude westerly jet would lead to errors in Rossby wave propagation and teleconnection patterns forced by ENSO, resulting in an inaccurate anomaly forecast. Therefore, it is important to reduce the model bias.

The verification data are the ERA-5 reanalyses for 2-meter air temperature (T2m) and 200-hPa zonal wind (U200), the Global Precipitation Climatology Project (GPCP; Huffman et al. 2009) dataset for precipitation, and the NOAA Optimum Interpolation (OI) Sea Surface Temperature V2 (Reynolds et al. 2002) for SST. The systematic error presented here is for the 1-month lead seasonal mean, averaged over the 12 initialization months.

We first look at the model bias of SST, which is shown in Figure 1. As can be seen, CanCM4i is doing a good job in controlling the model drift, with biases only in limited areas near the west coast of South America, east coast of East Asia and North America, and along the tropical Pacific and high latitude North Atlantic and Southern oceans (Figure 1a). On the other hand, GEM5-NEMO better represented the coastal regions of East Asia, southwest Africa and northwest of Southern America, despite its systematic cold biases in the tropical oceans (Figure 1b). GEM5-NEMO is also showing a dipole pattern of eastern coast of North America.

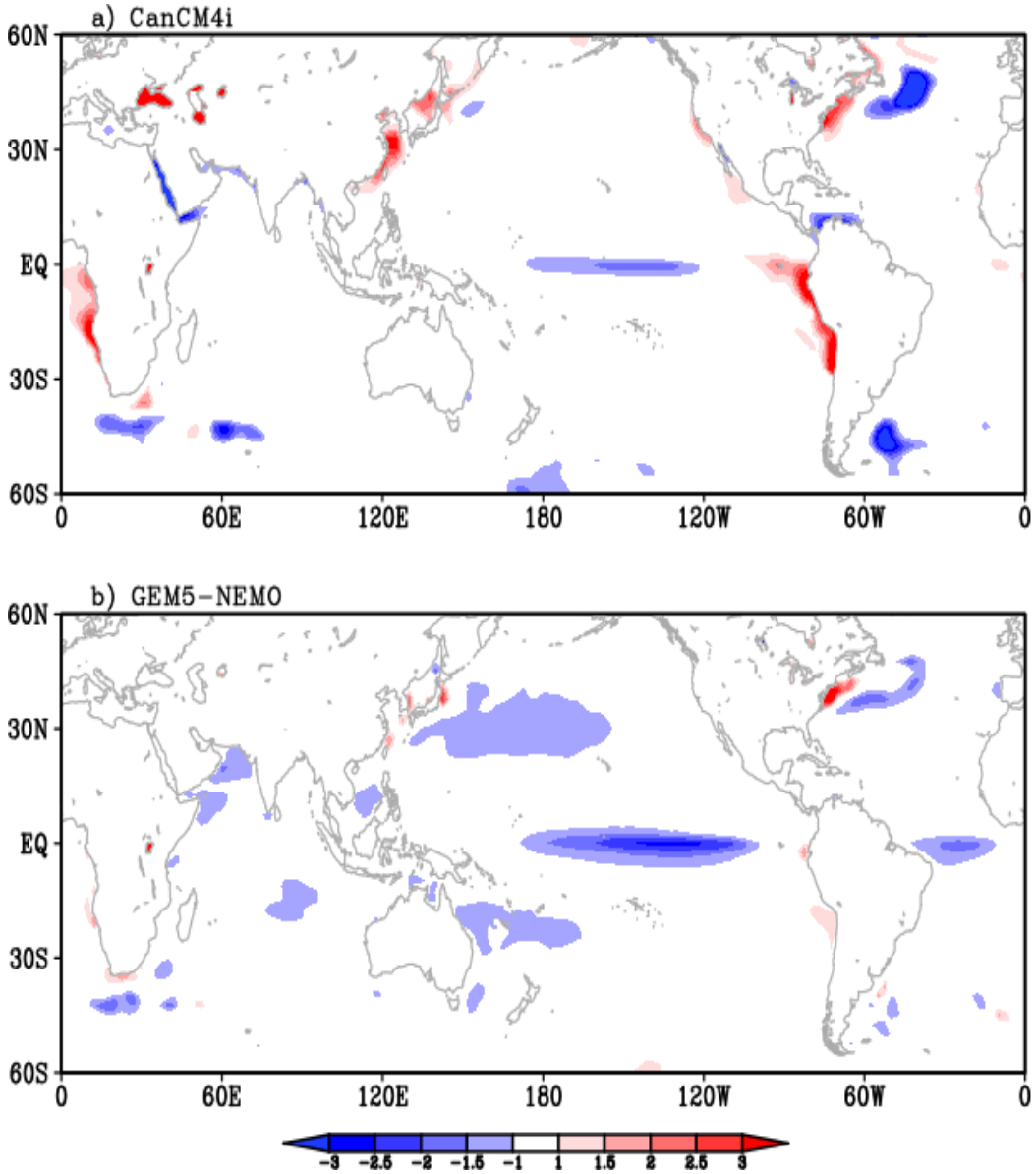


Figure 1. Seasonal mean SST systematic error at one-month lead averaged for all 12 initialization months a) for CanCM4i, and b) for GEM5-NEMO.

Figure 2 shows the geographical distribution of systematic error for T2m. The CanCM4i model is seen to have quite strong cold biases over the Northern Hemisphere Polar Region (Figure 2a), that may be related to the treatment of sea ice physics, or atmospheric physics over sea ice. Furthermore, it has warm T2m biases over the Northern middle-high latitude continents and over South America and cold biases over the mountains regions. GEM5-NEMO, on the other hand, is

predominantly showing cold bias, particularly over mountainous regions and. Over the ocean, CanCM4i shows some warm biases near the west coast of South America, east coast of East Asia and North America. Cold biases are observed in GEM5-NEMO in the tropical Pacific, which are related to the SST biases as discussed above.

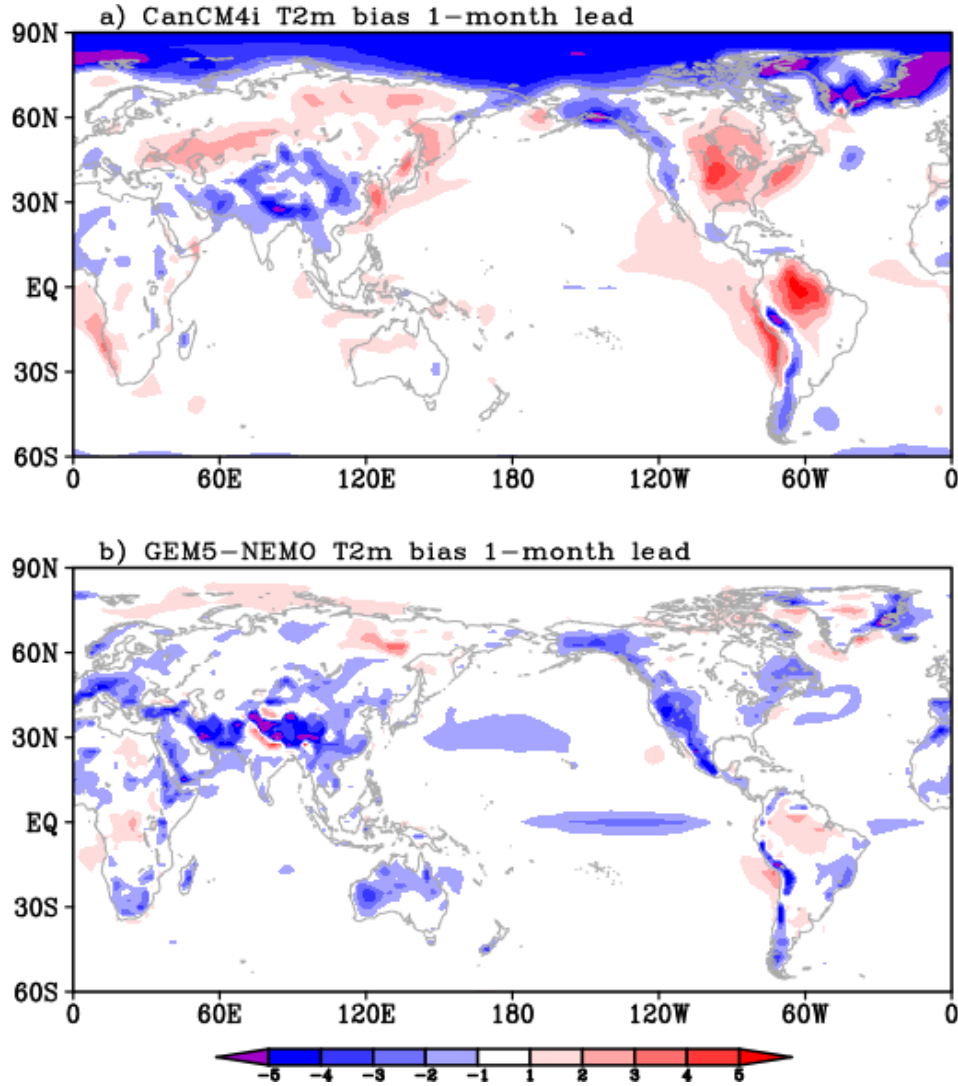


Figure 2. Seasonal mean T2m systematic error at 1-month lead for CanCM4i (top) and GEM5-NEMO (bottom). Unit: °C.

Shown in Figure 3 is the systematic error in precipitation rate. The two models seem to have a similar precipitation bias distribution. Excessive precipitation is found over a large area of the

tropics with insufficient precipitation over the equatorial Pacific, a feature of the double–intertropical convergence zone (ITCZ) which is common to many coupled general circulation models (e.g., Lin 2007). CanCM4i has a strong wet bias in the tropical Indian Ocean in addition to the bias over west Pacific. In GEM5-NEMO, the bias is stronger of western Pacific compared to Indian Ocean. Over the tropical South American continent, CanCM4i has a stronger dry bias than GEM5-NEMO. Over North America, the bias in GEM5-NEMO is also less compared to CanCM4i

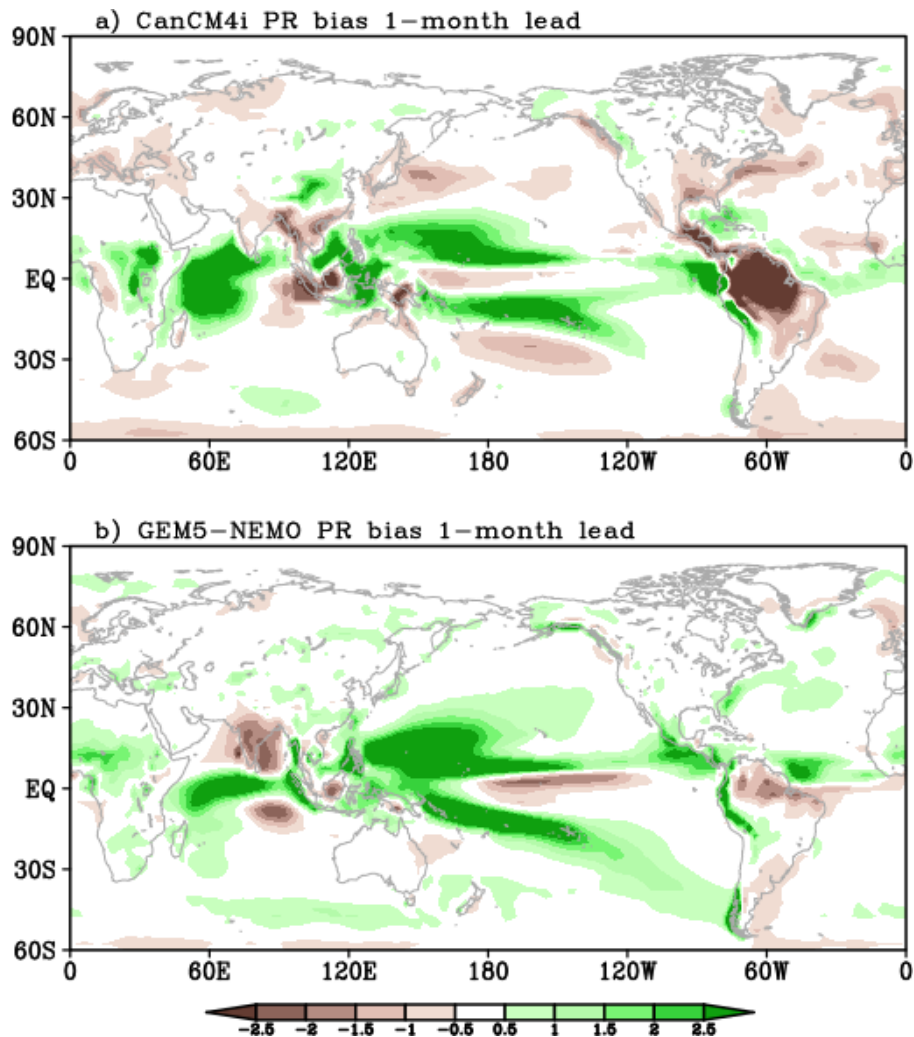


Figure 3. Precipitation systematic error at 1-month lead for CanCM4i (top) and GEM5-NEMO (bottom). Unit: mm/day.

Many previous studies have discussed the importance of the extratropical zonal westerly flow for Rossby wave propagation (e.g., Hoskins and Ambrizzi, 1993). The systematic error of U200 is illustrated in Figure 4. The two models have quite different distributions of U200 bias in the extratropical regions. CanCM4i tends to have overestimated westerlies in the Northern Hemisphere middle latitudes, whereas GEM5-NEMO has less zonal wind systematic errors.

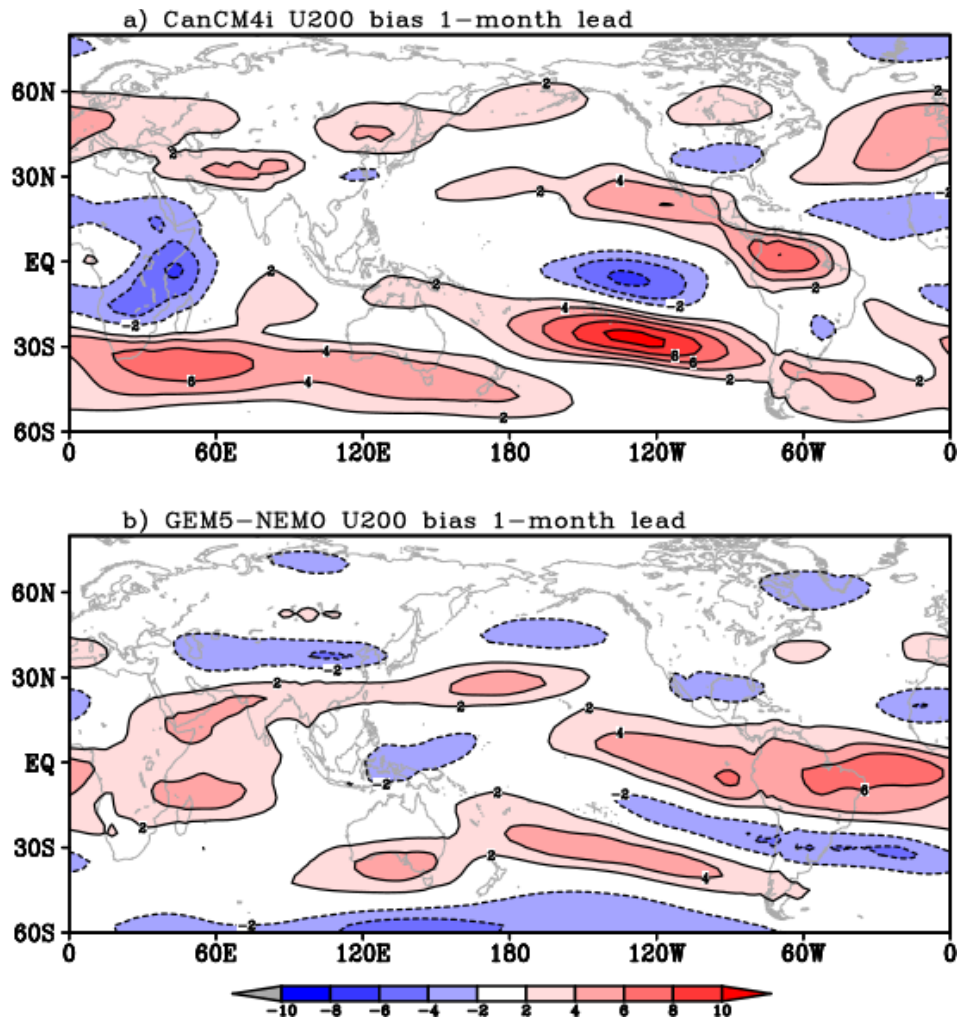


Figure 4. Systematic errors of 200 hPa zonal wind at 1-month lead for CanCM4i (top) and GEM5-NEMO (bottom). Unit: m/s.

6 Skill evaluation of CanSIPSv2.1 comparing to CanSIPSv2

The performance of CanSIPSv2.1 is evaluated in comparison with CanSIPSv2 for the hindcast period. The verification data used are the ERA-5 reanalysis for air temperatures and geopotential height, and the GPCP V2.3 dataset for precipitation.

The skill measures considered are for deterministic forecasts, determined from the ensemble mean of the predicted anomalies. In addition to the global maps for winter and summer forecasts, we consider area averages (over the globe, global land, North America and Canada for temperature and precipitation, over the globe, the Northern Hemisphere extratropics, tropics and Southern Hemisphere extratropics for 500-hPa geopotential height) of anomaly correlation, i.e. the correlation coefficient between predicted and observed anomalies. In addition, in assessing the ensemble forecast skill over Canada, we also discuss the continuous ranked probability skill score (CRPSS; e.g., Bradley and Schwartz 2011) which measures differences between the forecast and observed probabilistic distributions. Below is a comparison of the skills of the two systems for various variables.

Please note that the verification period used in CanSIPSv2 is 1981-2010, whereas 1991-2020 period is used for CanSIPSv2.1 to reflect the change of hindcast period in IC3. For bar graphs and head to head comparison of GEM5-NEMO with GEM4-NEMO, the same verification period of 1981-2010 is used.

6.1 Surface air temperature

Figure 5 shows the global geographical distribution of anomaly correlation skill for predictions of seasonal mean surface air temperature from the CanSIPSv2 hindcasts (left) and the new CanSIPSv2.1 hindcasts (right), for the DJF season with zero-month lead. As is usually the case the highest skill for both systems is in the tropics and especially the tropical Pacific, where SST anomalies are most persistent and ENSO imparts relatively high predictability. Skills are also appreciable in many locations over land, including most of North America where much of the seasonal predictability particularly in winter and early spring is attributable to the teleconnected influence of ENSO. In general, the skill distributions of the two systems are comparable. The

global average skill of CanSIPSv2.1 is higher than CanSIPS2. Similar conclusion can be obtained for the JJA season (Figure 6), as well as other seasons (not shown).

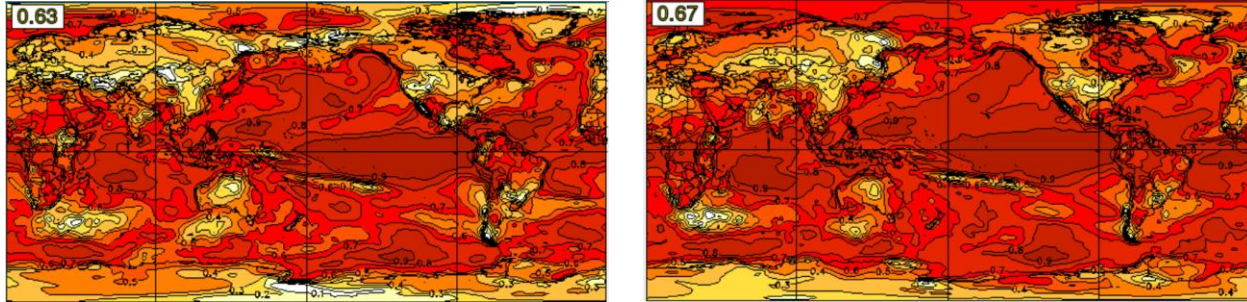


Figure 5. Geographical distribution of anomaly correlation skill for predictions of seasonal mean DJF near-surface air temperature at zero month lead, for the CanSIPSv2 (left) and CanSIPSv2.1 (right), based on the 1981-2010 historical forecast period for CanSIPSv2 and the 1991-2020 period for CanSIPSv2.1. Verification data is ERA-5. Globally averaged skills are marked in the upper-left corner of each panel.

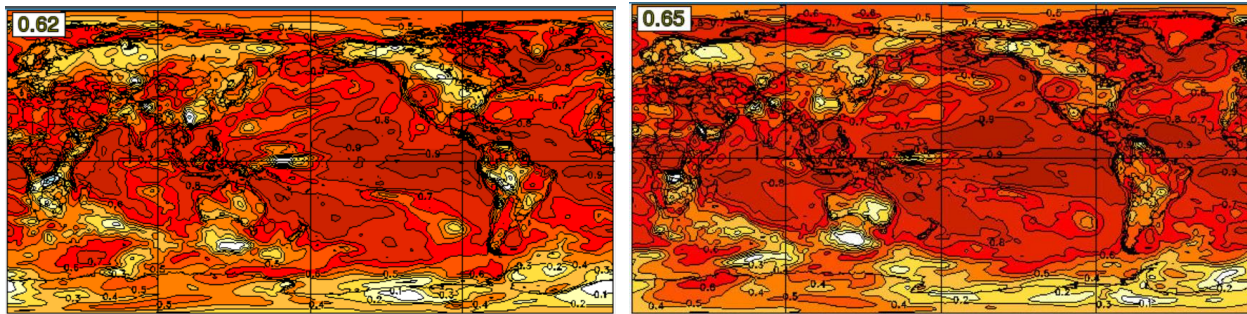


Figure 6. Same as Figure 5, but for JJA.

Shown in Figure 7 are T2m anomaly correlation skills for different regions and for different lead times averaged over all the 12 initialization months. It is evident that CanSIPSv2.1 has a performance better than that of CanSIPSv2 on global scale as well as for tropical regions at all lead times, though the difference is not statistically significant for the longer lead times. While the skill of CanSIPSv2.1 is similar to CanSIPSv2 over Canada at 0 month lead time, CanSIPSv2.1 shows a slightly better performance at selected longer lead times.

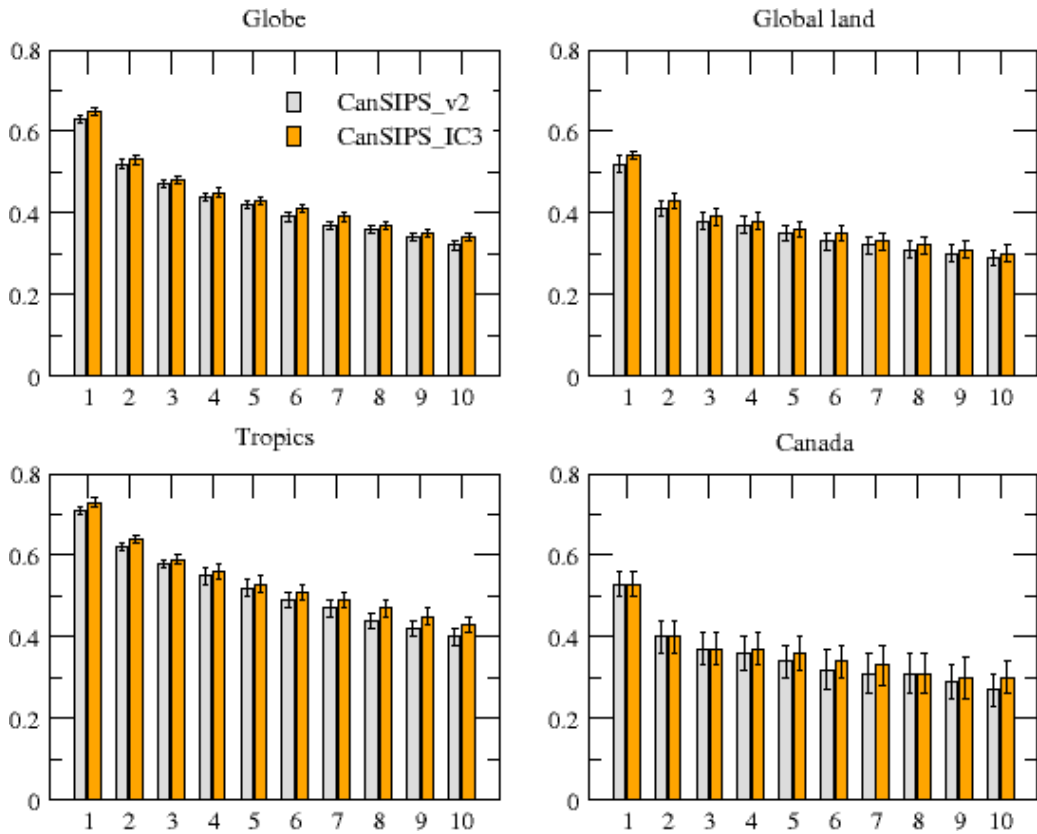


Figure 7. Anomaly correlation skills for hindcasts of seasonal mean near-surface air temperature as a function of lead times for CanSIPSV2 and CanSIPSV2.1 (CanSIPS_IC3). The skills shown are averages for all 12 initialization months. The verification is against the ERA-5 reanalysis for the period of 1981-2010. The horizontal axis indicates forecast season number, i.e., season 1 for months 1-3, season 2 for months 2-4... and season 10 for months 10-12.

To measure the quality of probability forecasts of the ensemble system, we present in Figure 8 the continuous ranked probability skill score (CRPSS) for DJF seasonal mean T2m forecast at zero month lead in Canada. In both CanSIPSV2 and CanSIPSV2.1, high skill scores are observed in a large part of northeast Canada and the west coastal regions. Relatively low skill is seen over the Prairies and over Northwest Territories for CanSIPSV2 and CanSIPSV2.1 respectively. The CRPSS skill distribution is consistent with the anomaly correlation of the ensemble mean forecast as shown in Figure 5. Comparing the two systems, it is clear that CanSIPSV2.1 performs better than the previous CanSIPSV2, especially in eastern Canada. Similar feature of the CRPSS skill scores

can be seen for JJA (Figure 9). It is also observed that the skill is improved in CanSIPSV2.1 comparing to CanSIPSV2.

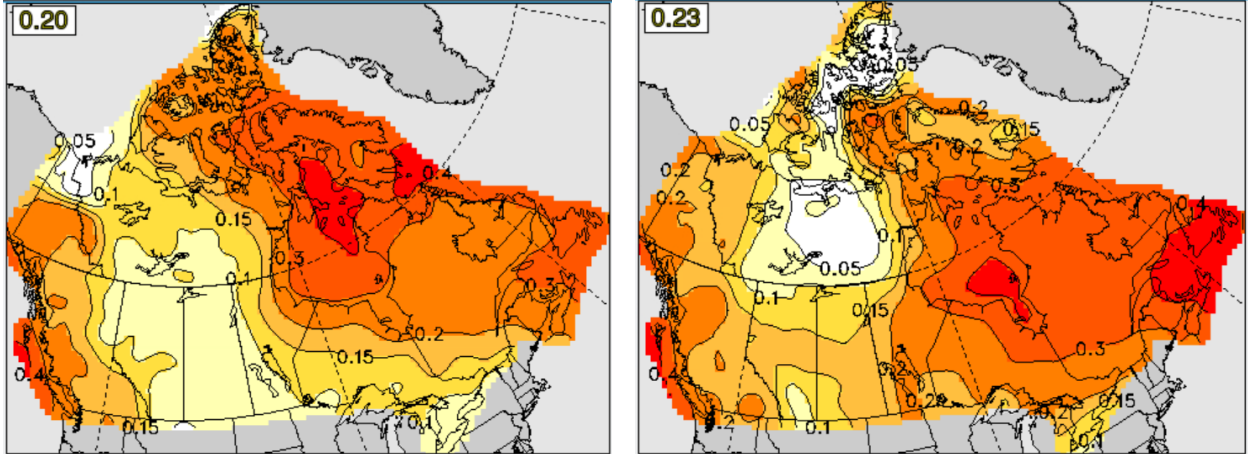


Figure 8. CRPSS skill for seasonal mean DJF near-surface air temperature at zero month lead, for the CanSIPSV2 (left) and CanSIPSV2.1 (right), based on the 1981-2010 historical forecast for CanSIPSV2 and the 1991-2020 historical forecast for CanSIPSV2.1. Verification data is ERA-5. Globally averaged skills are marked in the upper-left corner of each panel.

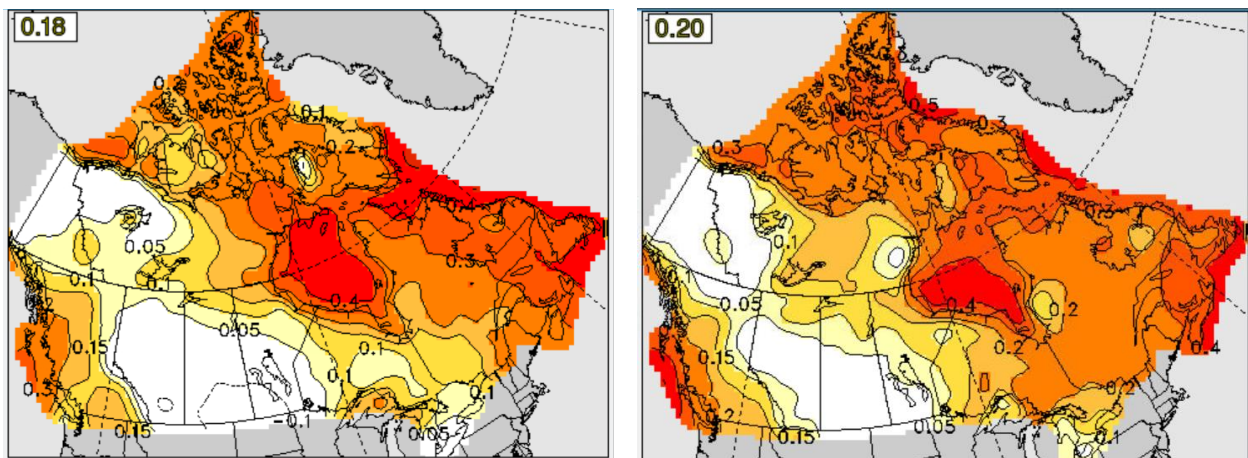


Figure 9. Same as Figure 8, but for JJA.

6.2 Precipitation

The global distribution of anomaly correlation skill for seasonal mean precipitation forecast in DJF with zero-month lead is shown in Figure 10 for CanSIPSv2 (left) and CanSIPSv2.1 (right) hindcasts. Again, high skill is mainly observed in the tropical regions, reflecting the contribution of ENSO. Some skill of precipitation is seen in the western and eastern coastal regions of North America. The global average skill of CanSIPSv2.1 is higher than CanSIPSv2, although the distributions of the two systems are very similar. For the JJA forecast, the precipitation skill has a similar distribution as DJF but with a weaker magnitude (Figure 11). In this season, both systems produce skillful seasonal precipitation forecasts over western North America. Again, the global average skill of precipitation in CanSIPSv2.1 is higher than that of CanSIPSv2.

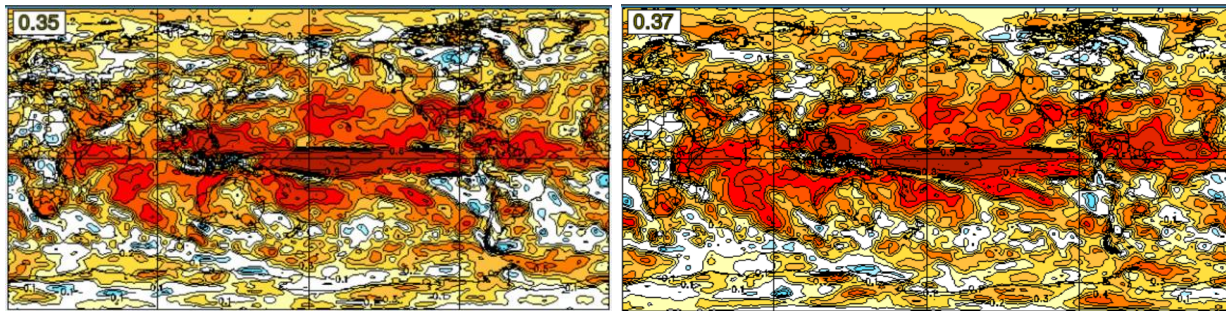


Figure 10. Geographical distribution of anomaly correlation skill for predictions of seasonal mean DJF precipitation at zero month lead, for the CanSIPSv2 (left) and CanSIPSv2.1 (right), based on the 1981-2010 historical forecast for CanSIPSv2 and the 1991-2020 forecast period for CanSIPSv2.1. Verification data is GPCP V2.3. Globally averaged skills are marked in the upper-left corner of each panel.

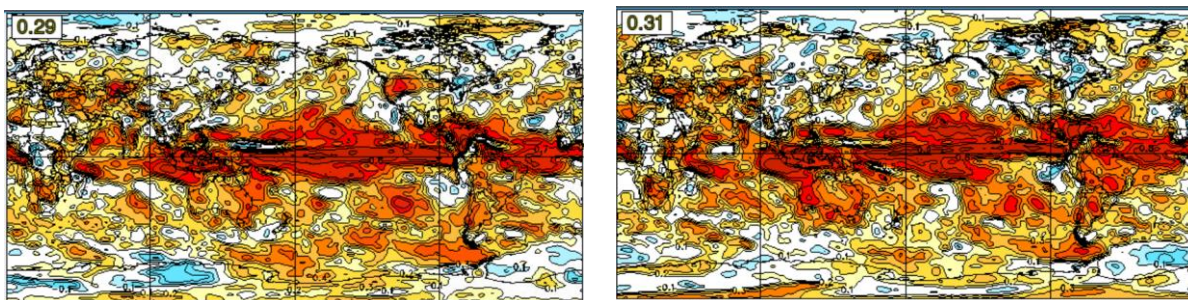


Figure 11. Same as Figure 10, but for JJA.

The anomaly correlation skills of precipitation averaged over all 12 initialization months for different regions are illustrated in Figure 12 for lead times of 1 to 10 months. Here the comparison is made between GEM4-NEMO (Operational) and GEM5-NEMO (IC3). In general, the precipitation skill is low for both systems, particularly over Canada. Furthermore, the skill in all regions drops substantially after lead month one. It is seen that GEM5-NEMO is superior to GEM4-NEMO in precipitation forecast in all regions at longer lead times, especially in the tropics. This likely results from the improvement of ENSO skill as is discussed in 6.4.

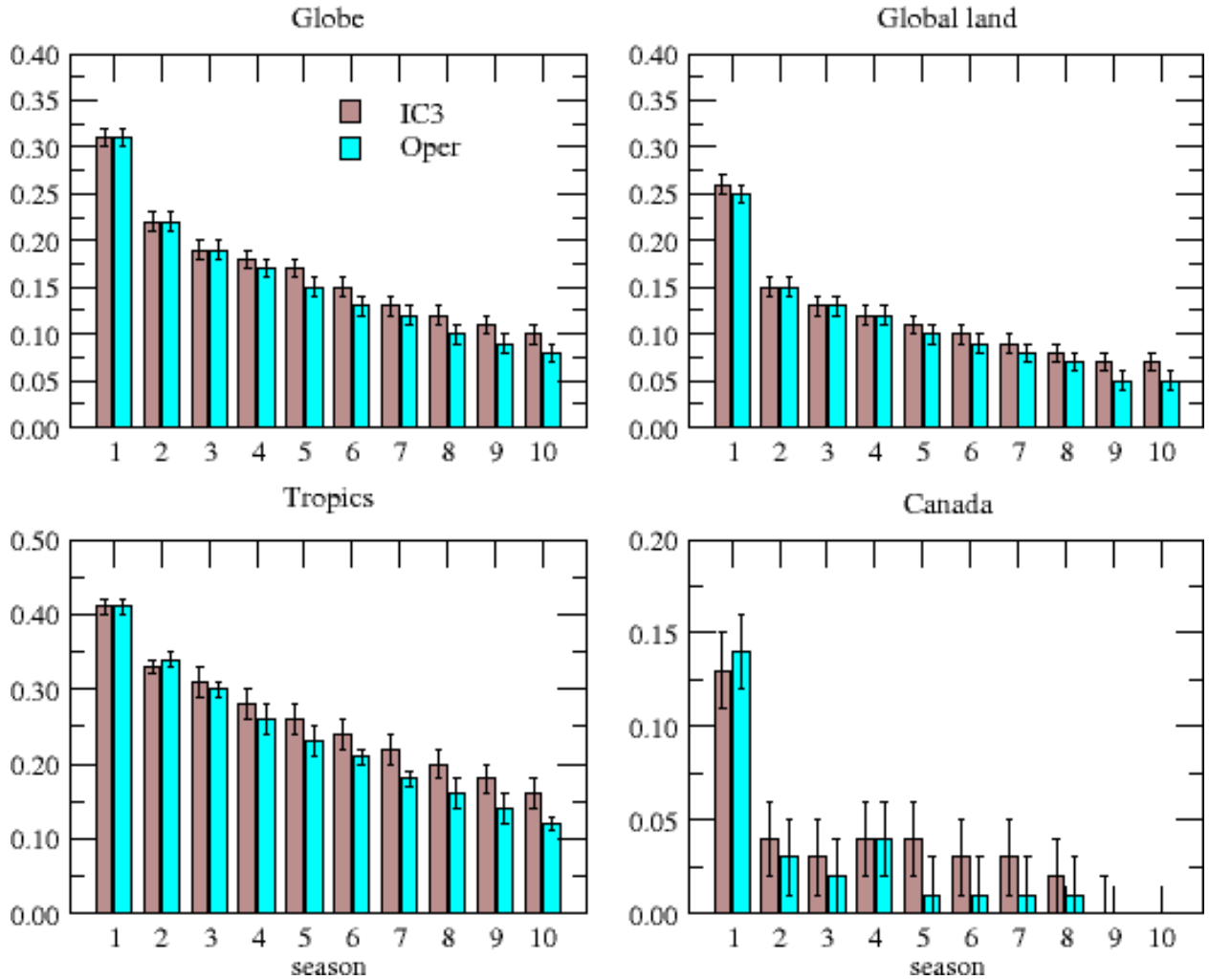


Figure 12. Anomaly correlation skills for hindcasts of seasonal mean precipitation as a function of lead times for GEM4-NEMO (Operational) and GEM5-NEMO (IC3). The skills shown are averages for all 12 initialization months. The verification is against GPCP V2.3 during 1981-2010.

The horizontal axis indicates forecast season number, i. e., season 1 for months 1-3, season 2 for months 2-4... and season 10 for months 10-12.

The CRPSS skills for DJF and JJA seasonal mean precipitation forecasts at zero month lead over Canada are shown in Figure 13 and Figure 14, respectively. It is evident that the precipitation forecast skill is low in both systems. CanSiPSv2.1 is showing a slight degradation in skill in both seasons, which is unlikely statistically significant consistent with the bottom-left panel of Fig. 12.

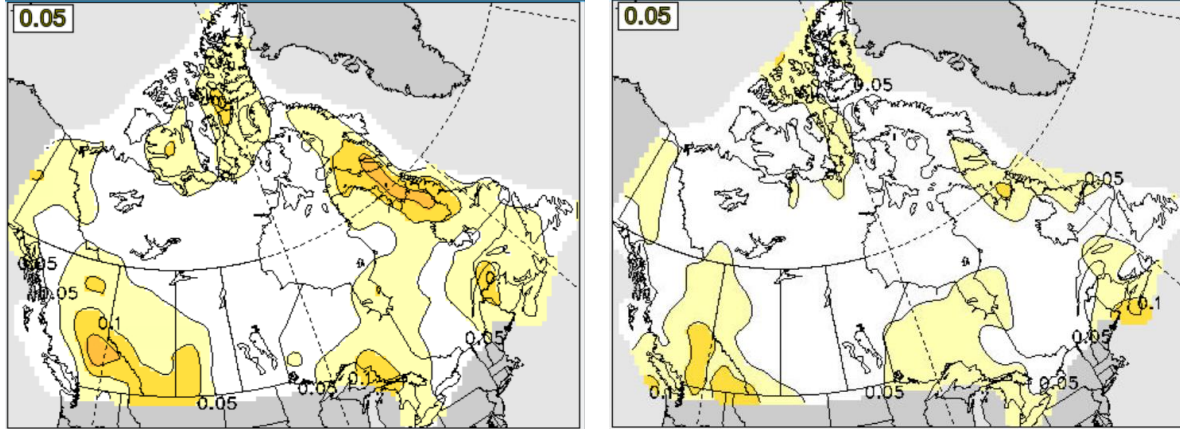


Figure 13. CRPSS skill for seasonal mean DJF precipitation at zero month lead, for the CanSiPSv2 (left) and CanSiPSv2.1 (right), based on the 1981-2010 forecast period for CanSiPSv2 and the 1991-2020 forecast period for CanSiPSv2.1. Verification data is GPCP V2.3. Globally averaged skills are marked in the upper-left corner of each panel.

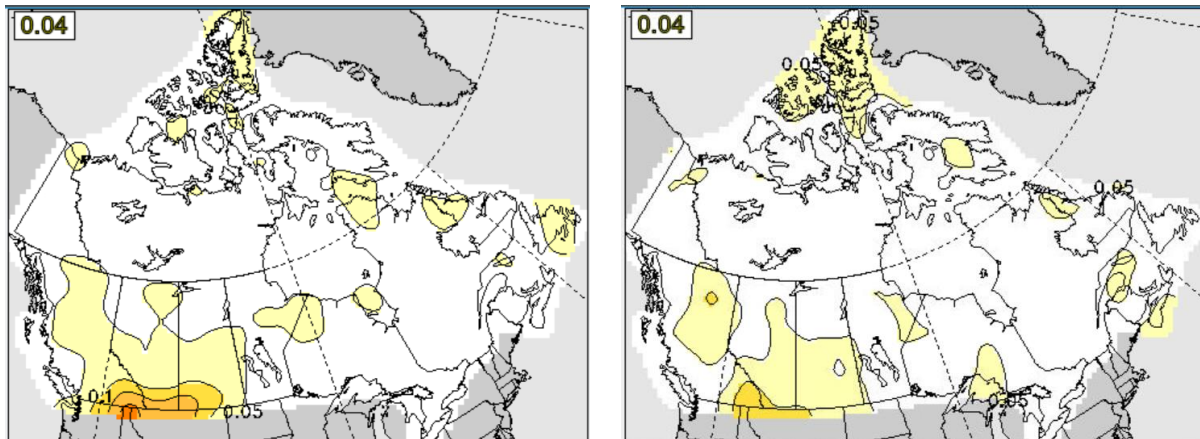


Figure 14. Same as Figure 13, but for JJA.

6.3 500-hPa geopotential height

In this section, we evaluate the seasonal forecast skill of 500-hPa geopotential height (Z500). Spatial distributions of the forecast skill for zero lead for the winter season (DJF) and summer season (JJA) are presented.

The anomaly correlation skills for DJF seasonal mean Z500 at zero month lead are compared between CanSIPSv2 and CanSIPSv2.1 in Figure 15. Similar to T2m and precipitation, significant skill of Z500 is found in the tropics. In the Northern Hemisphere extratropics, the correlation skill is high over the North Pacific and most part of Canada, resulting from variability of the PNA associated with ENSO (e.g., Wallace and Gutzler 1981). Relatively high correlation skills are also observed over Greenland and the middle latitude North Atlantic, which appears related to the NAO. In general, the two systems have a similar skill distribution. However, the skill at global average is higher in CanSIPSv2.1 than in CanSIPSv2.

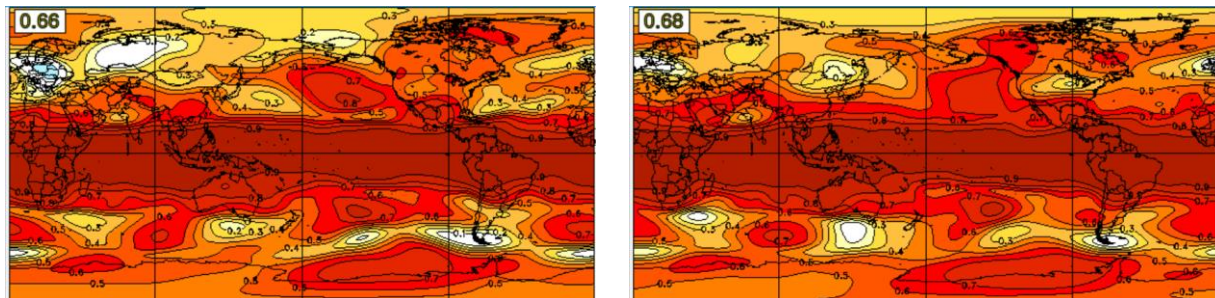


Figure 15. Geographical distribution of anomaly correlation skill for seasonal mean DJF 500-hPa geopotential height at zero month lead, for the CanSIPSv2 (left) and CanSIPSv2.1 (right), based on the 1981-2010 forecast period for CanSIPSv2 and the 1991-2020 forecast period for CanSIPSv2.1. Verification data is ERA-5 reanalysis. Globally averaged skills are marked in the upper-left corner of each panel.

For the season of JJA, as can be seen in Figure 16, the forecast skill of seasonal mean Z500 is also high in the tropics. In the Northern Hemisphere extratropics, besides the Greenland and polar regions, four centres of high skill are found in a wave pattern along the middle latitudes, that are eastern Europe, China, the North Pacific and western North America. The last is likely responsible for the high temperature and precipitation skills in western North America as seen in Figure 6 and

Figure 11. CanSIPSv2.1 has a slightly higher global average of skill value than CanSIPSv2, although the two systems have a very similar skill distribution.

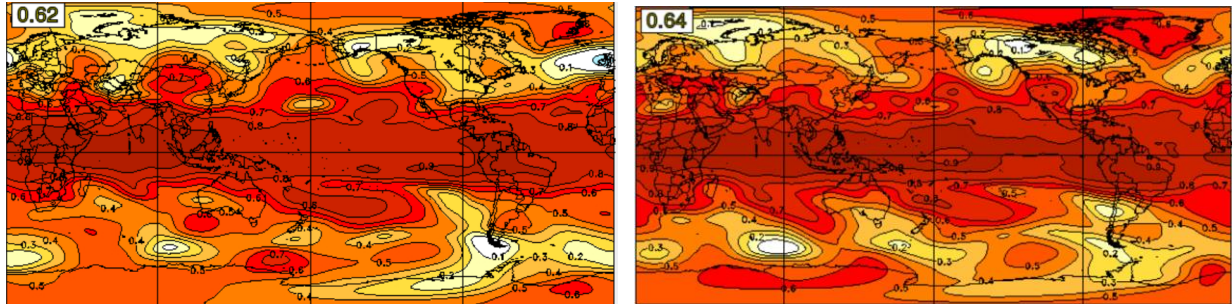


Figure 16. Same as Figure 15, but for JJA.

The anomaly correlation skill averaged over all 12 initialization months for different regions, i.e., the globe, the Northern Hemisphere extratropics (30N-90N), the tropics (30S-30N) and the Southern Hemisphere extratropics (30S-90S), are presented in Figure 17 for GEM4-NEMO and GEM5-NEMO. The two systems in general have comparable correlation skill of ensemble mean Z500.

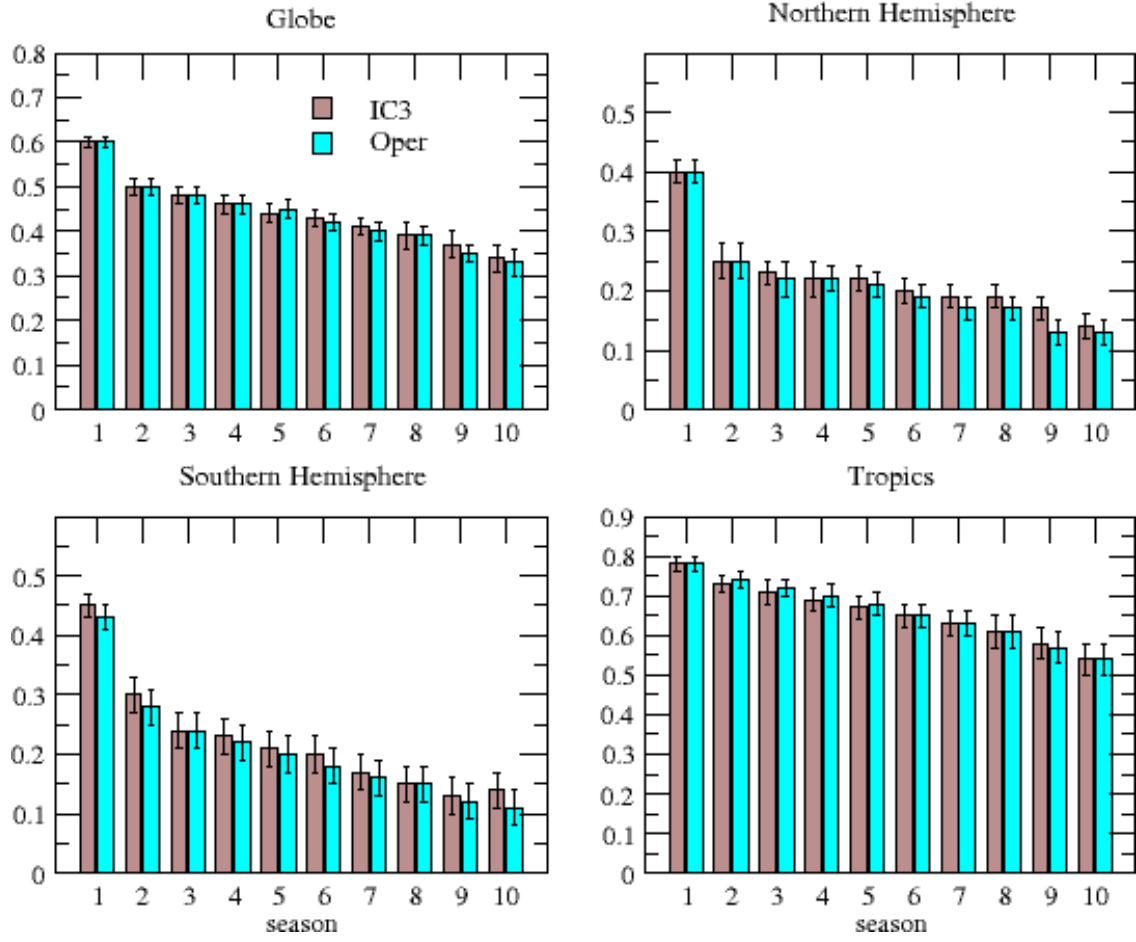


Figure 17. Same as Figure 12 but for seasonal mean Z500. The skills shown are averages for all 12 initialization months over the globe, the Northern Hemisphere extratropics (30° - 90° N), the tropics (30° S- 30° N), and the Southern Hemisphere extratropics (90° S- 30° S). The verification is against ERA5 during 1981-2010.

In order to see the probabilistic skill evolution with the increase of lead time, shown in Figure 18 is the Z500 continuous ranked probability score (for which lower values indicate higher skill) averaged over the globe, northern extratropics, tropics, and southern extratropics as a function of lead time. The skills shown are averages for all 12 initialization months. As can be seen, the improvement of forecast skill of GEM5-NEMO over that of GEM4-NEMO occurs for longer lead times for all regions except for the tropics.

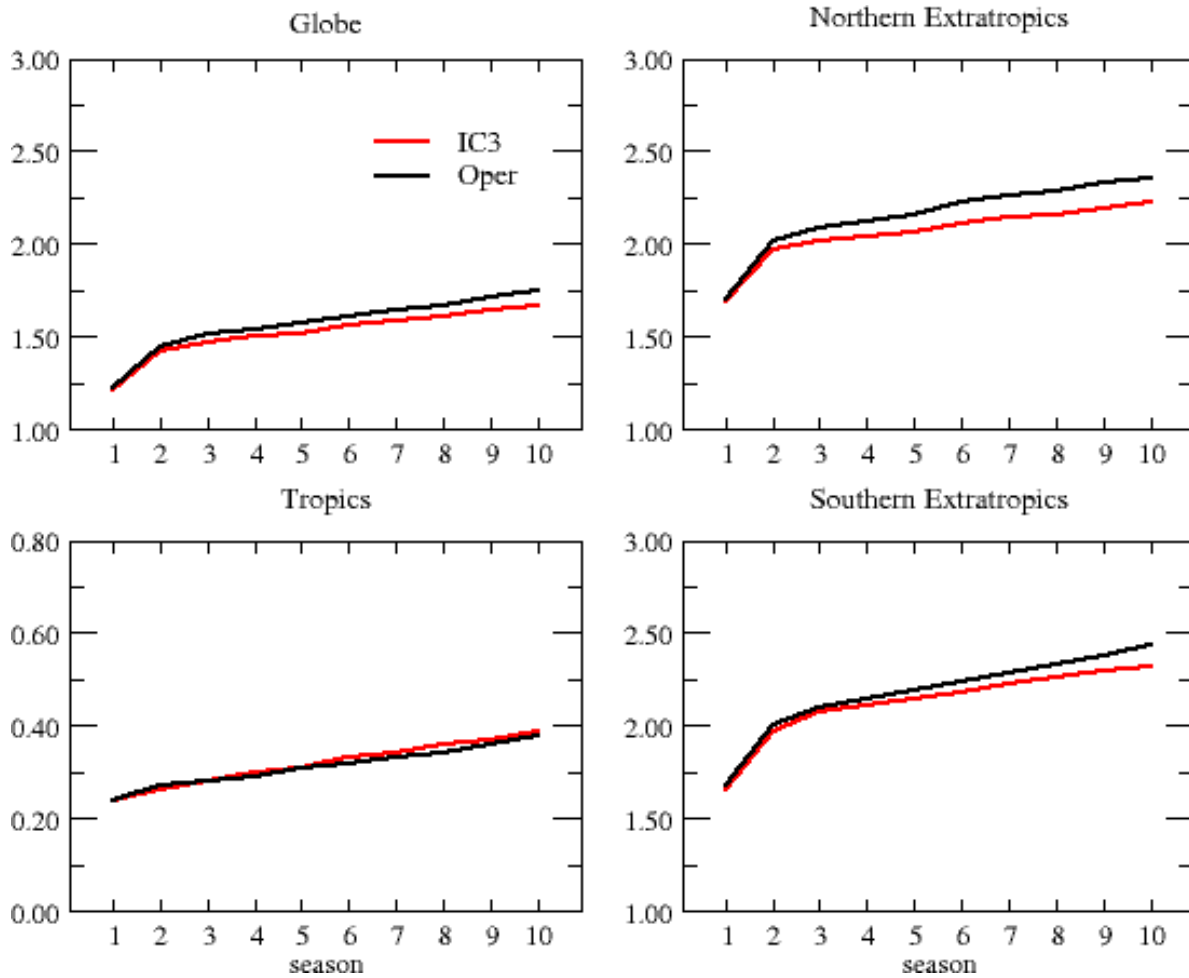


Figure 18. Continuous Ranked Probability Score (CRPS) for seasonal mean Z500 as a function of lead time averaged over the globe (top left), northern extratropics (top right), tropics (bottom left) and southern extratropics (bottom right). The skills shown are averages for all 12 initialization months during 1981-2010.

6.4 SST and ENSO

We first show the anomaly correlation skill of DJF seasonal mean SST at one-month lead, i.e., initialized on November 1, in Figure 19. The two systems have a very similar skill distribution. High skill of SST forecast can be found over the global ocean, with the maximum skill in the ENSO region of the equatorial eastern Pacific. The global average skill of CanSIPSv2.1 (0.64) is higher than that of CanSIPSv2 (0.61). The skill for the one-month lead SST forecast of JJA has a similar distribution as in DJF, but it is less concentrated in the ENSO region (Figure 20).

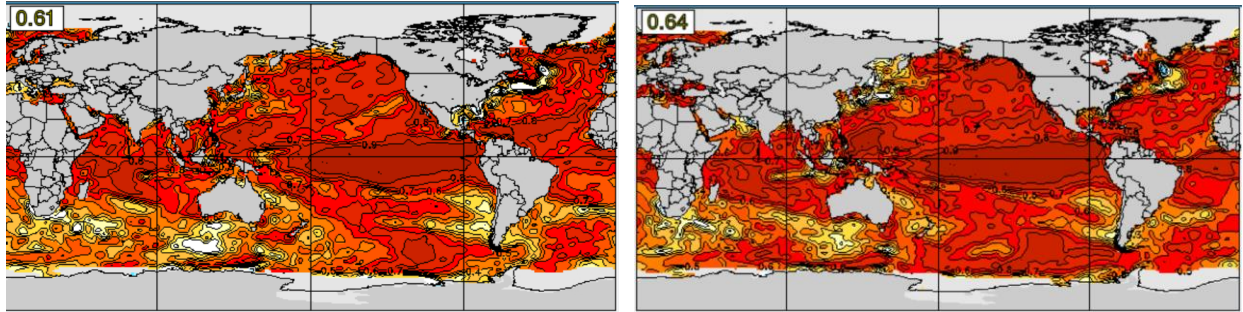


Figure 19. Anomaly correlation reforecast skill of DJF seasonal mean SST at one-month lead based on the 1981-2010 historical forecast period for CanSIPSv2 and the 1991-2020 period for CanSIPSv2.1. Verified against OISST. Left: CanSIPSv2, Right CanSIPSv2.1. The globally averaged skill is marked in the upper-left corner of each panel.

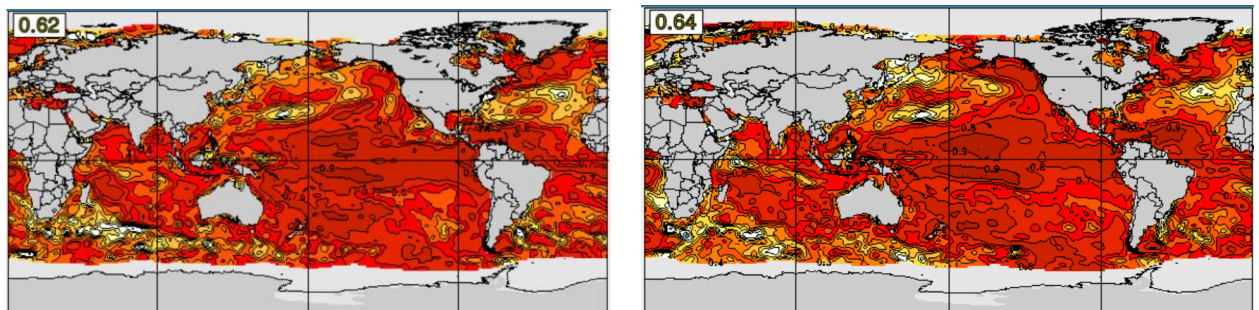


Figure 20. Same as Figure 19, but for JJA reforecast initialized on May 1.

To demonstrate the forecast skill of ENSO in GEM5-NEMO, the Nino3.4 index is used which is defined as the SST anomaly averaged in the area of 5°N-5°S, 170°W-120°W. Figure 21 provides a summary of the correlation skill of the monthly mean Nino3.4 index as a function of target month (horizontal axis) and lead time in month (vertical axis) for GEM5-NEMO and its predecessor

GEM4-NEMO. In general, the two systems have comparable ENSO forecast skill. GEM5-NEMO has a slightly better overall skill. For the winter target seasons, GEM5-NEMO shows a better performance. For example, for 0.9 correlation skill threshold for DJF and JFM forecasts, GEM5-NEMO can predict ENSO at that level of skill in a lead time of 6-months, which is about two months longer than GEM4-NEMO.

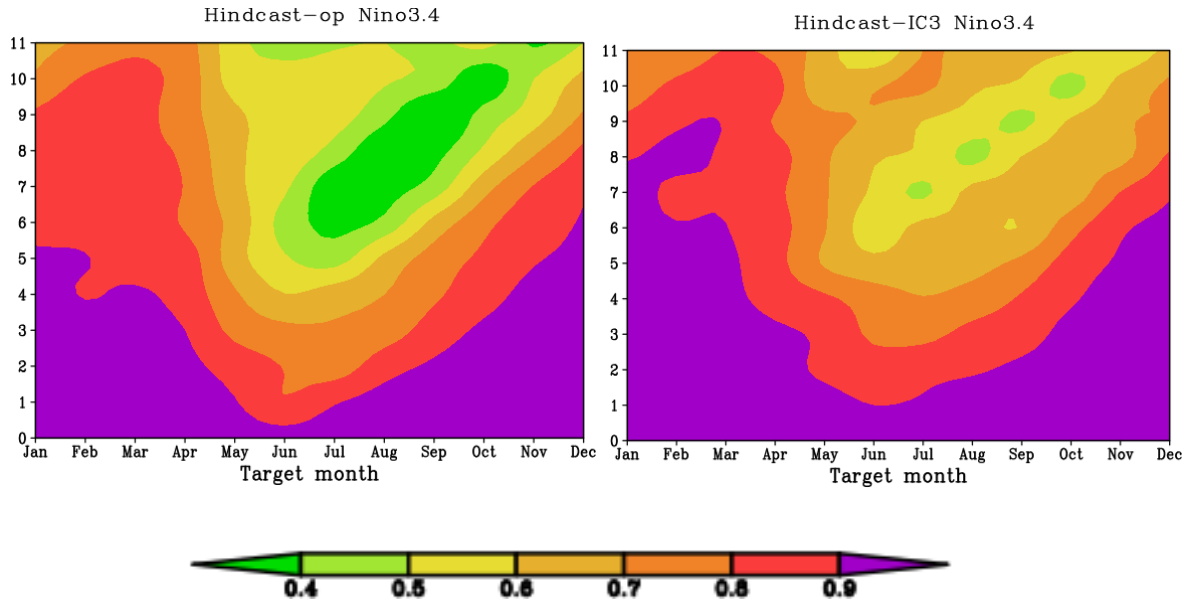


Figure 21. Anomaly correlation reforecast skill of seasonal mean Niño3.4 index as a function of target month (horizontal axis) and lead time (vertical axis). Left: GEM4-NEMO, Right GEM5-NEMO for the 1981-2010 period.

6.5 MJO

The skill of predicting Madden Julian Oscillation (MJO) is also shown to improve drastically from lead time of 17 days in the current operational system of GEM4-NEMO to around 30 days in the GEM5-NEMO version (Figure 22). This is quite a good performance compared to most of the existing sub-seasonal to seasonal (S2S) models (which are run at a higher resolution) and is much closer to the ECMWF S2S forecast system which has a lead time of around 32 days for predicting MJO skillfully.

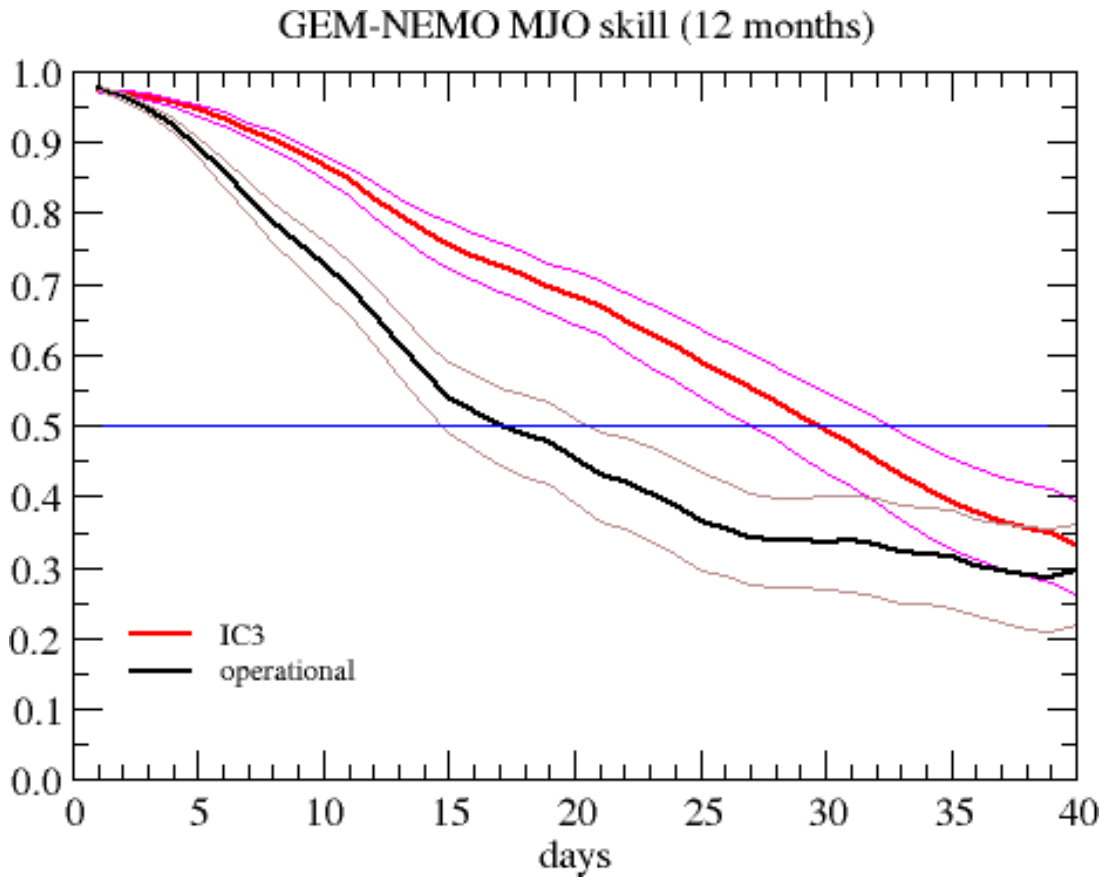


Figure 22: Forecast skill of MJO as a function of lead time for GEM5-NEMO and GEM4-NEMO using data during 1981-2010 period.

6.6 Sea ice

The first version of CanSIPS was one of the first seasonal prediction systems to have an interactive sea ice model component that in principle enables seasonal predictions of sea ice. In practice,

CanSIPS Arctic sea ice prediction skill, though appreciable, was attributable mainly to the long-term trend which however tended to be underrepresented in the reforecasts (Sigmond et al., 2013). This suggested considerable room for improvement, and in fact deficiencies in CanSIPS initialization of sea ice were identified that degraded skill. These included unrealistic Arctic sea ice extent trends in the data product used to initialize sea ice concentration in the reforecasts, as well as the use of a seasonally varying model-based climatology having no long-term thinning trend to initialize sea ice thickness.

A further deficiency of sea ice initialization in the CanSIPS reforecasts was that the sea ice concentration (SIC) product that was used was biased low compared to the GDPS analysis, especially during the summer melt season. This contributed to a notable high bias in real time CanSIPS forecasts of Arctic sea ice extent, which were not useful largely for that reason.

The modifications to the initialization of sea ice in the CanCM4i forecasts and reforecasts described in sections 3.1 and 4.1 were intended to address the above issues and to provide higher forecast skill for sea ice in CanCM4i compared to its predecessor, and to reduce the large biases and resulting errors in real time forecasts.

Improvement in sea ice skill in CanSIPSV2.1 is illustrated in Figure 23, which compares anomaly correlation reforecast skills for prediction of September SIC at four-month lead in CanSIPSV2 and CanSIPSV2.1.

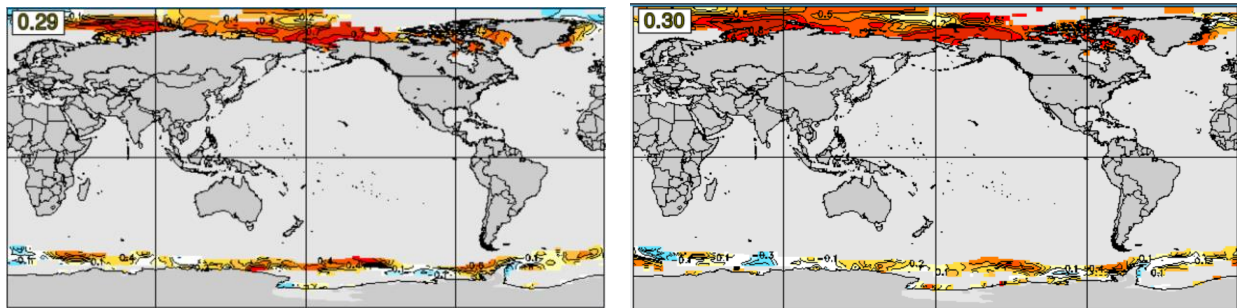


Figure 23. Anomaly correlation reforecast skill of September monthly mean SIC at four-month lead (initialized at the beginning of May) based on the 1981-2010 historical forecast period for CanSIPSV2 and the 1991-2020 period for CanSIPSV2.1, verified against Had2CIS. Left:

CanSIPSv2, Right: CanSIPSv2.1. The globally averaged skill over ice covered regions is marked in the upper-left corner of each panel.

6.7 Snow water Equivalent and soil moisture

Comparison of the performance of the new GEM5-NEMO and its predecessor for land surface variables such as snow water equivalent (SWE) and soil moisture, shown in Figure 24, indicate that GEM5-NEMO produce comparable or better performances. For instance, the skill of SWE prediction is improved over Eurasia and the improvement in soil moisture forecast is also evident over South America and Africa.

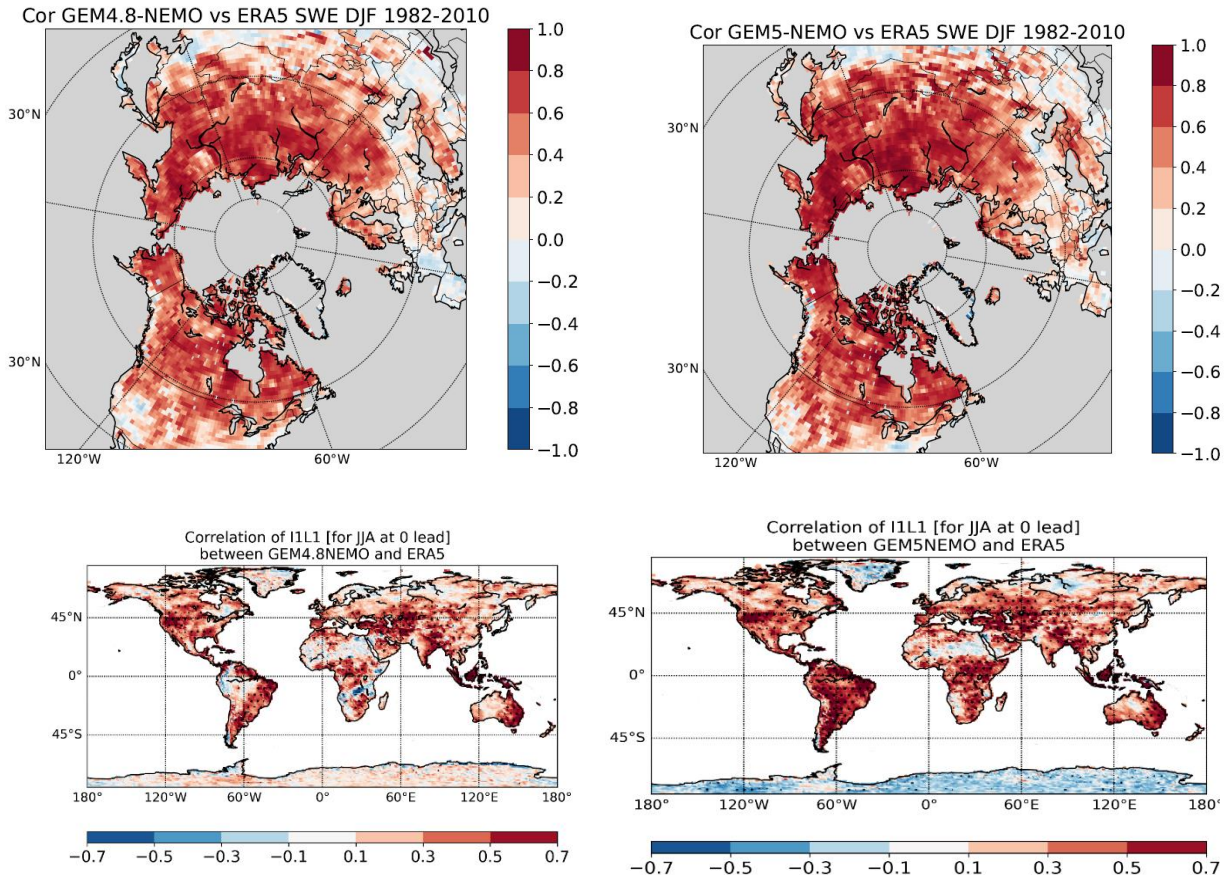


Figure 24: Spatial pattern of inter-annual correlation between ERA5 reanalysis vs GEM4-NEMO (left column) and GEM5-NEMO (right column) for snow water equivalent (top row) and top layer soil moisture (bottom row) based on the 1981/2-2010 period.

7 Qualitative evaluation of the parallel run

The parallel run since the beginning of October 2021 produced consistent seasonal forecasts with the operational CanSIPSV2. For instance, Figures 25 and 26 illustrate that the forecasts from the parallel runs based on CanSIPSV2.1 produced similar outlook of colder sea surface temperature over equatorial Pacific. Both forecasts are also indicating an east-west dipole pattern with colder anomaly over western Canada, possibly associated to the colder (La-Niña) conditions over equatorial Pacific Ocean.

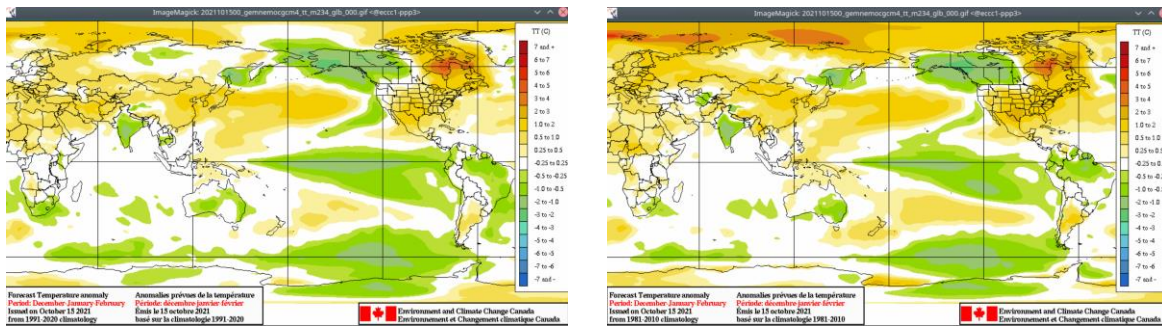


Figure 25. Deterministic seasonal forecast of temperature anomalies for DJF 2021/22 based on forecasts initialized on October 15, 2021 from parallel runs of CanSIPSV2.1 (left) and from operational runs of CanSIPSV2 (right).

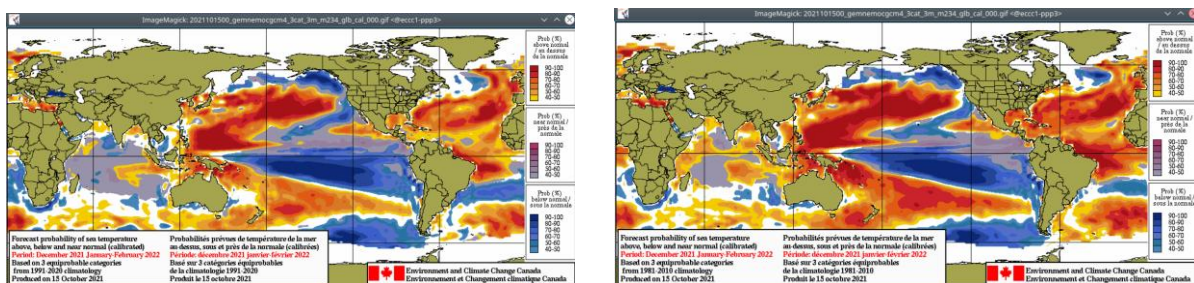


Figure 26. probabilistic categorical seasonal forecast of sea surface temperature for DJF 2021/22 based on forecasts initialized on October 15, 2021 from parallel runs of CanSIPSV2.1 (left) and from operational runs of CanSIPSV2 (right).

8 Details of implementation

An important aspect of any operational seasonal prediction system is that the same model versions and initialization methods are used for producing the forecasts and reforecasts, and both CanSIPSV2.1 models fulfill this requirement. However, because the MSC analyses employed for initializing the forecasts in real time are not available for the reforecast period, there are inevitably some differences between the data products used for initializing the forecasts and reforecasts, as described in sections 3 and 4. In general, the choice of data products for initializing the reforecasts is guided by considerations of compatibility with the corresponding analyses used in real time. For example, the ORAS5 ocean reanalysis used by both CanSIPSV2.1 models is formulated using the same modelling system (NEMO) and basic grid (ORCA025) as the GIOPS ocean analysis used for initialization in real time. Also, the Had2CIS sea ice concentration product was developed and chosen for initialization of the reforecasts for both models because it exhibits lower biases relative to the GPDS analysis employed in real time than other products such as ORAS5, which is substantially biased toward lower concentrations than the GPDS product especially in the summer melt season.

It is important to highlight that, one of the changes made in this innovation cycle is the alteration of the climatological hindcast period. This implies subsequent forecasts of CanSIPSV2.1 will be issued based on the hindcast climatology computed for the period of 1991-2020 as opposed to the 1981-2010 period. This implies that hindcast climatologies for monthly, mid-monthly, and seasonal forecast for all lead times are re-computed and changed during the operational implementation. The hindcast climatology for an unofficial mid-month monthly forecast valid from the 16th of the current month to the 15th of the following month is computed by a linear combination of the month in question and the next month at lead 0 i.e. 0.5* (current month at lead 0 + next month at lead 0).

An additional aspect of operational CanSIPSV2.1 that differs from the reforecasts is that, whereas reforecasts are initialized once per month at 00Z on the first day of each month, operational forecasts are initialized and run every day according to the following schedule, with initialization at 00Z in each case:

- 15th day of month: forecast through the remainder of the current month plus six additional months (i.e. six-month forecast with 0.5 month lead), which serves as a mid-month

“preview” forecast The hindcast climatology for the first mid-month monthly forecast at 0.5 month lead is calculated as 0.5^* (current month (lead 0) + next month (lead 0)).

- 4th to last day of month: 12-month forecast with 4-day lead, which serves as a backup in the event of an issue with the official forecast
- last day of month: 12-month forecast with 1-day lead, which serves as the official forecast
- every other day: forecast through the remainder of the current month plus one additional month, to track system functioning; hindcast climatologies are computed as linear interpolations between lead 0 of the current month and lead 0 of the next monthclimatologies , much as for the mid-month forecast.

Note in particular the 1-day lead time for the official forecasts (as compared to 0-day lead for the reforecasts), which ensures their timely delivery by the start of each month but is unlikely to have any measurable impact on seasonal forecast skill.

Probabilistic official forecast products are provided at

- https://weather.gc.ca/saisons/index_e.html
- <http://climate-scenarios.canada.ca/?page=seasonal-forecasts>

As for CanSIPS, these calibrated probabilistic forecasts are post-processed using the methodology described in Kharin et al. (2017). This improves the reliability of the forecasts, meaning that the forecast probabilities provide a fair measure of the chance of the forecast conditions actually occurring, rather than being over- or under-estimated, as determined from the reforecasts.

Computational time Requirement for GEM5-NEMO

Comparison of computational time requirement indicated that GEM5-NEMO takes 4 hours and 20 minutes to complete 12 month integration (c.f. 1 hour and 30 minutes for the current system) on the U1 supercomputer. This increase in computing time is attributed to the new system’s higher spatial resolution and reduced model time step. To avoid a single task in maestro suite from running for too long, a new feature is added in GEM5-NEMO maestro suite with a capability of chunking it into two time-slots. This new feature of splitting the model integration, does not increase the speed of the model simulation. However, in the event that the model crashes during

the final stage of the computation, it allows to re-start the forecast from the second time slice rather than from the beginning.

9 Summary

The main aspects of the CanSIPSV2.1 system are summarized as follows.

- Like CanSIPSV2, CanSIPSV2.1 employs two global atmosphere-ocean-sea ice coupled models to produce multi-model ensemble seasonal predictions. One of the climate models in CanSIPSV2, GEM4-NEMO was replaced by GEM5-NEMO. The remaining climate model in CanSIPSV2.1, CanCM4i is left as is.
- For CanSIPSV2.1 the hindcast climatology is computed based on the 1991-2020 period, whereas for CanSIPSV2, the 1981-2010 period was used.
- CanSIPSV2.1 outperforms CanSIPSV2 in forecasting surface air temperature in all regions for all lead times.
- The forecast skill of precipitation is low, GEM5-NEMO has better skill for seasonal mean precipitation forecast at longer lead time than GEM4-NEMO.
- The SST and ENSO skill is also improved in CanSIPSV2.1 comparing to CanSIPSV2, especially for the Northern Hemisphere winter seasons.
- The forecast skill of the MJO is significantly improved in GEM5-NEMO comparing to GEM4-NEMO.
- Improvement of sea ice forecast quality is achieved in CanSIPSV2.1 comparing to the previous system.

10 Acknowledgements

Members of the Seasonal Forum and many colleagues at RPN, CCCma and CMC contributed to the development and implementation of CanSIPSV2.1. In particular, we would like to thank the following colleagues for their various contributions to this project:

Frédéric Dupont, François Roy, Jean-François Lemieux, Jean-Marc Bélanger, Normand Gagnon, Peter Houtekamer, Ron McTaggart-Cowan, Ayrton Zadra, Paul Vaillancourt, Michel Roch, Stéphane Chamberland, Vivian Lee, Michel Desgagné, Stéphane Bélair, Maria Abrahamowicz, Marco Carrera, Nicola Gasset, Katja Winger.

11 References

- Bechtold, P., E. Bazile, [F. Guichard](#), [P. Mascart](#), and [E. Richard](#), 2001: A mass-flux convection scheme for regional and global models. *Q. J. R. Meteorol. Soc.*, 127, 869–886. <https://doi.org/10.1002/qj.49712757309>.
- Bernier, N. B., and S. Bélair, 2012: High horizontal and vertical resolution limited-area model: Near-surface and wind energy forecast applications, *J. Appl. Meteorol. Climatol.*, **51**, 1061–1078.
- Bradley, A. A., and S. S. Schwartz, 2011: Summary verification measures and their interpretation for ensemble forecasts, *Mon. Wea. Rev.*, **139**, 3075–3089.
- Carrera, M. L., S. Bélair, V. Fortin, B. Bilodeau, D. Charpentier, and I. Doré (2010), Evaluation of snowpack simulations over the Canadian Rockies with an experimental hydrometeorological modeling system, *J. Hydrometeorol.*, 11, 1123–1140.
- Charron, M., R. Frenette and N. Gagnon, 2011: First Operational Implementation of the Regional Ensemble Prediction System at CMC (REPS 1.0.0).
- Côté, J., S. Gravel, A. Méthot, A. Patoine, M. Roch, and A. Staniforth, 1998: The operational CMC-MRB Global Environmental Multiscale (GEM) model. Part I: Design considerations and formulation. *Mon. Wea. Rev.*, **126**, 1373–1395.
- Dee, D. P., and Co-authors, 2011: The ERA-Interim reanalysis: configuration and performance of the data assimilation system. *Q. J. R. Meteorol. Soc.*, 137, 553–597.
- Derome, J., Brunet, G., Plante, A., Gagnon, N., Boer, G. J., Zwiers, F. W., Lambert, S. and Ritchie, H. 2001. Seasonal predictions based on two dynamical models. *Atmosphere-Ocean*, 39: 485–501.
- Dirkson, A., W. J. Merryfield and A. H. Monahan, 2017: Impacts of sea ice thickness initialization on seasonal Arctic sea ice predictions. *J. Climate*, 30, 1001–1017, doi:10.1175/JCLI-D-16-0437.1.

Gagnon, N., and Co-authors, 2015: Improvements to the Global Ensemble Prediction System (GEPS) from version 4.0.1 to version 4.1.1. Canadian Meteorological Centre Technical Note. [Available on request from Environment Canada, Centre Météorologique Canadien, division du développement, 2121 route Transcanadienne, 4e étage, Dorval, Québec, H9P1J3 or via the following web site :

http://collaboration.cmc.ec.gc.ca/cmc/cmoi/product_guide/docs/lib/technote_geps-411_20151215_e.pdf

Gauthier, P., M. Buehner, and L. Fillion, 1999: Background-error statistics modelling in a 3D variational data assimilation scheme: Estimation and impact on the analyses. Proc. ECMWF Workshop on Diagnosis of Data Assimilation Systems, Reading, United Kingdom, ECMWF, 131–145.

Hersbach, H., Bell, B., Berrisford, P., Hirahara, S., Horányi, A., Muñoz-Sabater, J., Nicolas, J., Peubey, C., Radu, R., Schepers, D. and Simmons, A., 2020. The ERA5 global reanalysis. *Quarterly Journal of the Royal Meteorological Society*, 146(730), pp.1999-2049.

Hoskins, B. J., and T. Ambrizzi, 1993: Rossby wave propagation on a realistic longitudinally varying flow. *J. Atmos. Sci.*, **50**, 1661-1671.

Houtekamer, P.L., Mitchell H. L. and Deng X. 2009: Model Error Representation in an Operational Ensemble Kalman Filter, *Mon. Wea. Rev.*, **137**, 2126-2143.

Hunke, E.C. and Lipscomb, W.H.. 2010. CICE: the Los Alamos sea ice model, documentation and software user's manual, Version 4.1. Los Alamos, NM, Los Alamos National Laboratory. (Tech. Rep. LA-CC-06-012.)

Huffman, G. J., R. F. Adler, D. T. Bolvin, and G. Gu, 2009: Improving the global precipitation record: GPCP Version 2.1, *Geophys. Res. Lett.*, 36, L17808, doi:10.1029/2009GL040000.

Ioannidou, L., W. Yu, and S. Bélair, 2014: Forecasting of surface winds over Eastern Canada using the Canadian offline land surface modeling system, *J. Appl. Meteorol. Climatol.*, **53**, 1760–1774, doi:10.1175/JAMC-D-12-0284.1.

- Kain, J. S., and J. M. Fritsch, 1990: A one-dimensional entraining detraining plume model and its application in convective parameterization. *J. Atmos. Sci.*, 47, 2784-2802.
- Kim, G., and Coauthors, 2016: Global and regional skill of the seasonal predictions by WMO Lead Centre for Long-Range Forecast Multi-Model Ensemble. *Int. J. Climatol.*, 36, 1657–1675, <https://doi.org/10.1002/joc.4449>.
- Kharin, V. V., Q. Teng, F. W. Zwiers, G. J. Boer, J. Derome, J. S. Fontecilla, 2009 : Skill assessment of seasonal hindcasts from the Canadian Historical Forecast Project. *Atmos. Ocean.*, 47, 204-223.
- Kharin, V. V., W. J. Merryfield, G. J. Boer, W.-S. Lee, 2017: A postprocessing method for seasonal forecasts using temporally and spatially smoothed statistics. *Mon. Wea. Rev.*, 145, 3545-3561, doi:10.1175/MWR-D-16-0337.1.
- Kirtman, B. P., and Coauthors, 2014: The North American Multimodel Ensemble: Phase-1 seasonal-to-interannual prediction; phase-2 toward developing intraseasonal prediction. *Bull. Amer. Meteor. Soc.*, 95, 585–601, doi:<https://doi.org/10.1175/BAMS-D-12-00050.1>.
- Lin, H., N. Gagnon, S. Beauregard, R. Muncaster, M. Markovic, B. Denis, and M. Charron, 2016: GEPS based Monthly Prediction at the Canadian Meteorological Centre. *Mon. Wea. Rev.*, DOI: <http://dx.doi.org/10.1175/MWR-D-16-0138.1>.
- Lin, J.-L., 2007: The double-ITCZ problem in IPCCAR4 coupled GCMs: ocean-atmosphere feedback analysis. *J. Climate*, 20, 4497-4525.
- McFarlane, N.A., G.J. Boer, J.-P. Blanchet, and M. Lazare, 1992: The Canadian Climate Centre second-generation general circulation model and its equilibrium climate. *J. Climate*, 5, 1013-1044.
- Merryfield, W. J., W.-S. Lee, G. J. Boer, V. V. Kharin, J. F. Scinocca, G. M. Flato, R. S. Ajayamohan, J. C. Fyfe, Y. Tang, and S. Polavarapu, 2013: The Canadian Seasonal to Interannual Prediction System. Part I: Models and Initialization, *Mon. Wea. Rev.*, 141 , 2910-2945, doi:10.1175/MWR-D-12-00216.1.

- Min, Y.-M., V. N. Kryjov, and S. M. Oh, 2014: Assessment of APCC multimodel ensemble prediction in seasonal climate forecasting: Retrospective (1983–2003) and real-time forecasts (2008–2013), *JGR Atmosphere*, 119, 12132-12150.
- Noilhan, J. and S. Planton, 1989: A Simple Parameterization of Land Surface Processes for Meteorological Models. *Mon. Wea. Rev.*, 117, 536–549.
- Noilhan, J., and J. F. Mahfouf, 1996: The ISBA land surface parameterisation scheme, *Global Planet. Change*, 13, 145–159.
- Reynolds, R.W., N.A. Rayner, T.M. Smith, D.C. Stokes, and W. Wang, 2002: An improved in situ and satellite SST analysis for climate. *J. Climate*, 15, 1609-1625.
- Ritchie, H., 1991: Application of the semi-Lagrangian method to a multilevel spectral primitive-equations model. *Quart. J. Roy. Meteor. Soc.*, **117**, 91-106.
- Scinocca, J.F., N.A McFarlane, M. Lazare, J. Li, 2008: The CCCma third generation AGCM and its Extension into the Middle Atmosphere. *Atmospheric Chemistry and Physics*, **8**, 7055-7074.
- Separovic, L., S. Z. Husain, W. Yu, and D. Fernig (2014), High-resolution surface analysis for extended-range downscaling with limited-area atmospheric models, *J. Geophys. Res. Atmos.*, **119**, 13,651–13,682, doi:10.1002/2014JD022387.
- Shabbar, A. and A. G. Barnston, 1996: Skill of seasonal climate forecasts in Canada using canonical correlation analysis. *Mon. Wea. Rev.*, 124, 2370-2385.
- Sigmond, M., J.C. Fyfe, G.M. Flato, V.V. Kharin and W. J. Merryfield, 2013: Seasonal forecast skill of Arctic sea ice area in a dynamical forecast system, *Geophysical Research Letters*, 40, 529-534, doi:10.1002/grl.50129.
- Smith, G.C., F. Roy, M. Reszka, D. Surcel Colan, Z. He, D. Deacu, J.-M. Belanger, S. Skachko, Y. Liu, F. Dupont, J.-F. Lemieux, C. Beaudoin, B. Tranchant, M. Drévillon, G. Garric, C.-E. Testut, J.-M. Lellouche, P. Pellerin, H. Ritchie, Y. Lu, F. Davidson, M. Buehner, M. Lajoie and A. Caya, 2016: Sea ice Forecast Verification in the Canadian Global Ice Ocean Prediction System. *Quart. J. Roy. Met. Soc.*, 142, 659–671, doi: 10.1002/qj.2555.

Titchner, H. A., and N. A. Rayner (2014), The Met Office Hadley Centre sea ice and sea surface temperature data set, version 2: 1. Sea ice concentrations, *J. Geophys. Res. Atmos.*, 119, 2864-2889, doi: 10.1002/2013JD020316.

Zuo, H., Balmaseda, M. A., Tietsche, S., Mogensen, K., and Mayer, M.: The ECMWF operational ensemble reanalysis–analysis system for ocean and sea ice: a description of the system and assessment, *Ocean Sci.*, 15, 779–808, <https://doi.org/10.5194/os-15-779-2019>, 2019.

Appendix A List of Acronyms

GEM5-NEMO	Version 5 of GEM coupled with NEMO
CanCM3/4	CCCma Coupled Climate Model, versions 3/4
CanCM4i	CCCma Coupled Climate Model, versions 4, with improved initialization
CanSIPS	Canadian Seasonal to Interannual Prediction System
CanSIPSV2	CanSIPS version 2
CanSIPSV2.1	CanSIPS version 2.1
CCA	Canonical Correlation Analysis
CCCma	Canadian Centre for Climate Modeling and Analysis
CIS	Canadian Ice Service
CICE	Community of Ice Code
CMC	Canadian Meteorological Centre
CONCEPTS	The Canadian Operational Network of Coupled Environmental Prediction Systems
CRPSS	Continuous Rank probability Skill Score
ECCC	Environment and Climate Change Canada
EnKF	Ensemble Kalman Filter
ENSO	El Niño/Southern Oscillation
GDPS	Global Deterministic Prediction System
GEM	Global Environmental Multiscale model
GEM-NEMO	GEM and NEMO coupled model
GEM4-NEMO	GEM version 4 and NEMO coupled model used in CanSIPSV2
GEM5-NEMO	GEM version 5 and NEMO coupled model used in CanSIPSV2.1
GEPS	Global Ensemble Prediction System
GIOPS	Global Ice Ocean Prediction System
GOSSIP	Globally Organized System for Simulation Information Passing
GPCP	Global Precipitation Climatology Project
Had2CIS	HadISST2 combined with CIS digitized sea ice charts

HadISST2	Hadley Centre Sea Ice and Sea Surface Temperature Version 2
HFP	Historical Forecast Project
NEMO	Nucleus for European Modelling of the Ocean
MSC	Meteorological Service of Canada (of Environment Canada)
NAO	North Atlantic Oscillation
NCAR	National Center for Atmospheric Research
NCEP	(United States) National Centers for Environmental Prediction
NOAA	National Oceanic and Atmospheric Administration
NWP	Numerical Weather Prediction
PNA	Pacific/North American pattern
OISST	Optimum Interpolation Sea Surface Temperature of NOAA
ORAP5	Ocean Reanalyses Prototype 5
ORAS5	Ocean Reanalysis System 5
RPN	Recherche en Prévision Numérique
REOF	Rotated Empirical Orthogonal Function
SIC	Sea Ice Concentration
SPS	Surface Prediction System
SST	Sea Surface Temperature
T2m	2-meter air temperature
Z500	500-hPa geopotential height